2013

Design of Heat Exchangers for Cooling Low Temperature Flue Gas

Rinosh Polavarapu
Lehigh University

Design of Heat Exchangers for Cooling Low Temperature Flue Gas

by

Rinosh Polavarapu

A Thesis
Presented to the Graduate and Research Committee
of Lehigh University
in Candidacy for the Degree of
Master of Science

in

Mechanical Engineering & Mechanics

Lehigh University

May 2013

APPROVAL SHEET

This thesis is accepted and approved in partial fulfillment of the requirements for the Master of Science in Mechanical Engineering.

Design of Heat Exchangers for Cooling Low Temperature Flue Gas

Rinosh Polavarapu

_____

Date Approved

_____

Dr. Edward K. Levy
Thesis Advisor
Energy Research Center,
Lehigh University

_____

Dr. Gary Harlow
Department Chair Person
Department of Mechanical Engineering & Mechanics
Lehigh University

ACKNOWLEDGEMENTS

I would like to express my sincere gratitude to my thesis advisor Dr. Edward K. Levy for his valuable guidance and insight into Energy research. I lack words that could adequately thank Dr. Levy for helping me to complete thesis. The study was conducted at Energy Research Center of Lehigh University. I would like to thank Dr. Harun Bilirgen, Mr Joshua Charles and Mr Nipun Goel of the Energy Research Center for their guidance and valuable discussions regarding the project. Sincere thanks are due to Jodie Johnson and Ursla Levy of the Energy Research Center for making my research experience memorable throughout my life.

I would like to thank my family, Dhruthi Bearavolu & Dev Alapati for the inspiration and support they provided throughout the program.

TABLE OF CONTENTS

LIST OF FIGURES

LIST OF TABLES

ABSTRACT

Recovery of heat and moisture from the flue gas is the major criteria in designing the condensing heat exchanger. Apart from the condensation of moisture in flue gas, the condensation of sulfuric acid present in flue gas will also take place. A computer simulation code developed by previous Energy Research Center (ERC) researchers was modified to predict the condensation of sulfuric acid on tube walls of heat exchanger.

A computer simulation code was developed to predict the heat and mass transfer rates as well as required length of heat exchanger which is used as an evaporator in a power plant with Organic Rankine Cycle (ORC) unit. Simulations were performed to estimate the heat exchanger surface area, pressure drop and overall cost for installation and maintenance of heat exchangers in three different ORC units.

NOMENCLATURE

Symbol	*Interpretation*	*Units*
A_{eff}	Tube effective surface area	ft^2
A_i	Tube inner surface area	ft^2
A_{ic}	Tube inner surface area for one cell	ft^2
A_o	Tube outer surface area	ft^2
A_{oc}	Tube outer surface area for one cell	ft^2
C	Empirical coefficient depending on tube arrangement	-
$C_{p,cw}$	Specific heat of cooling water	BTU/lbm·°F
$C_{p,fg}$	Specific heat of flue gas	BTU/lbm·°F
D	Mass diffusivity	ft^2/hr
D_{H_2O-air}	Mass diffusivity of water vapor in air	ft^2/hr
D_{H_2O-gas}	Mass diffusivity of water vapor in flue gas	ft^2/hr
$D_{H_2SO_4-air}$	Mass diffusivity of sulfuric acid in air	ft^2/hr
$D_{H_2SO_4-gas}$	Mass diffusivity of sulfuric acid in flue gas	ft^2/hr
d_i	Tube inner diameter	in
d_o	Tube outer diameter	in
f	Friction factor	-
h_{cw}	Convective heat transfer coefficient for cooling water	BTU/hr·ft^2·°F
h_f	Convective heat transfer coefficient for condensate film	BTU/hr·ft^2·°F
h_{fg}	Convective heat transfer coefficient for wet flue gas	BTU/hr·ft^2·°F
$i_{cf,fg}$	Latent heat of Cooling fluid	BTU/lb
k_{cw}	Thermal conductivity of cooling water	BTU/hr·°F·ft
k_{fg}	Thermal conductivity of flue gas	BTU/hr·°F·ft
k_m	Mass transfer coefficient for water condensation	lb/mol·hr·ft^2
k_{m,H_2SO_4}	Mass transfer coefficient for sulfuric acid condensation	lb/mol·hr·ft^2
k_w	Thermal conductivity of tube material	BTU/hr·°F·ft
L	Length of tube	ft
L_g	Latent heat of water vapor	BTU/lb
$Le_{H_2SO_4-gas}$	Lewis Number of sulfuric acid in flue gas	-
Le_{H_2O-gas}	Lewis Number of sulfuric acid in flue gas	-
M_g	Molecular weight of wet flue gas	-

M_{H2SO4}	Molecular weight of Sulfuric acid	-
m	Empirical coefficient depending on tube arrangement	-
$\dot{m}_{cf}$	Mass flow rate of cooling fluid	lb/hr
$\dot{m}_{cd,H_2SO_4}$	Rate of condensation of sulfuric acid	lb/hr
$\dot{m}_{cw}/M_{cw}$	Mass flow rate of cooling water	lb/hr
$\dot{m}_{fg}/M_{FG}$	Mass flow rate of flue gas	lb/hr
N_L	Total number of tube rows	-
Nu_{cw}	Nusselt number for cooling water	-
Nu_{fg}	Nusselt number for flue gas	-
P_{atm}	Atmospheric Pressure	psi
P_{in}	Pressure of flue gas at the exit of exchanger	psi
P_{out}	Pressure of flue gas at the inlet of exchanger	psi
Pr	Prandtl number	-
Pr_s	Surface Prandtl number	-
P_{tot}	Total pressure of flue gas	psi
P_{cf}	Working fluid pressure in the evaporator	psi
q	Rate of heat transfer	BTU/hr
Q	Total volume flow rate of cooling water	ft^3/s
Re_{cw}	Reynolds number of cooling water	-
$Re_{cw,max}$	Maximum Reynolds number of cooling water	-
$Re_{fg,max}$	Maximum Reynolds number of flue gas	-
R_{fl}	Thermal resistance due to fouling on tube inner wall	hr·°F/BTU
$R_{flue\ gas}$	Thermal resistance of flue gas	hr·°F/BTU
r_i	Tube inner radius	in
r_o	Tube outer radius	in
R_{total}	Total thermal resistance of control volume	hr·°F/BTU
R_{wall}	Thermal resistance of tube wall	hr·°F/BTU
S_l	Longitudinal Pitch	in
S_t	Transverse pitch	in
T_{cw}	Mean temperature of cooling water	°F
T_{fg}	Mean temperature of flue gas	°F
T_i	Gas-condensate film interfacial temperature	°F
T_{ow}	Tube outer wall temperature	°F

U_0	Overall heat transfer coefficient	BTU/hr·ft2·°F
V_{avg}	Average velocity of water	ft/s
V_{max}	Maximum velocity of flue gas	ft/s
X_{cf}	Average quality of cooling fluid	-
y_{H2O}	Mole fraction of water vapor in the flue gas	vol%wet
yH_2SO_4	Mole fraction of sulfuric acid in the flue gas	vol%wet
y_i	Mole fraction of water vapor at the wall interface	vol%wet
$y_{i,H2SO4}$	Mole fraction of sulfuric acid at the wall interface	vol%wet

Greek Symbols :

α_{air}	Thermal diffusivity coefficient of air	ft^2/hr
α_g	Thermal diffusivity of flue gas	ft^2/hr
Δ	Difference or change	-
η	Efficiency	-
ε	Heat exchanger effectiveness	-
ρ	Density	lb/ft^3
ρ_{fg}	Density of flue gas	lb/ft^3
ρ_{cw}	Density of cooling water	lb/ft^3
χ	Pressure drop correction factor	-
γ	Specific heat ratio	-

1. INTRODUCTION

1.1 Condensation of Sulfuric Acid present in Flue Gas

Sulfur dioxide (SO_2) is usually one of the components present in flue gas formed from burning coal or oil. The sulfur dioxide content in flue gas is dependent on type and quality of fuel used in a power plant. Sulfur dioxide is one of the major gases that lead to the formation of acid rain.

The emission of sulfur dioxide from thermal power plants has to be controlled. Most of the utilities have either switched to use low sulfur coal or have installed scrubbers in order to control SO_2 emissions. More than 30% of the coal-fired power plants in U.S. already have FGD systems installed and operating. The number may be doubled over the next few years as existing regulations are implemented and proposed regulations are adopted (1).

The formation process of sulfuric acid from the sulfur present in coal is given below:

Initially sulfur present in the coal is burned to produce sulfur dioxide

$$S\ (solid) + O_2\ (gas) \rightarrow SO_2\ (gas)$$

Then, sulfur dioxide is oxidized to sulfur trioxide using excess oxygen from air

$$2\ SO_2\ (gas) + O_2(gas) \rightarrow 2\ SO_3(gas)$$

The sulfur trioxide is hydrated into sulfuric acid using the moisture present in flue gas

SO_3 (gas) + H_2O (gas) → H_2SO_4 (gas)

Finally, condensation of vaporized sulfuric acid to liquid sulfuric acid will occur on a surface when the surface temperature falls below the dew point temperature of sulfuric acid vapor.

H_2SO_4 (gas) → H_2SO_4 (liquid)

In this study, the sulfuric acid condensation rates on the tubes of heat exchangers have been investigated for different inlet mole fractions of sulfuric acid and moisture in the flue gas.

1.2 Organic Rankine Cycle

Large quantities of waste heat energy are discharged by industrial processes in flue gas from boilers and heaters. An efficient recovery of this waste heat might imply huge savings in fuel costs. Organic Rankine cycle (ORC) technology is one of the methods of recovering waste heat from flue gas at low temperatures. Similar to the Rankine cycle with steam, an Organic Rankine Cycle (ORC) is a closed-loop and continuous cycle. The important apparatus used in an ORC system is: a heat exchanger/vaporizer in which working fluid is vaporized, a turbine/generator to generate power from the expansion of vaporized fluid, a condenser to condense the expanded fluid back to a liquid and a working fluid pump to drive the fluid back into the heat exchanger. (2)

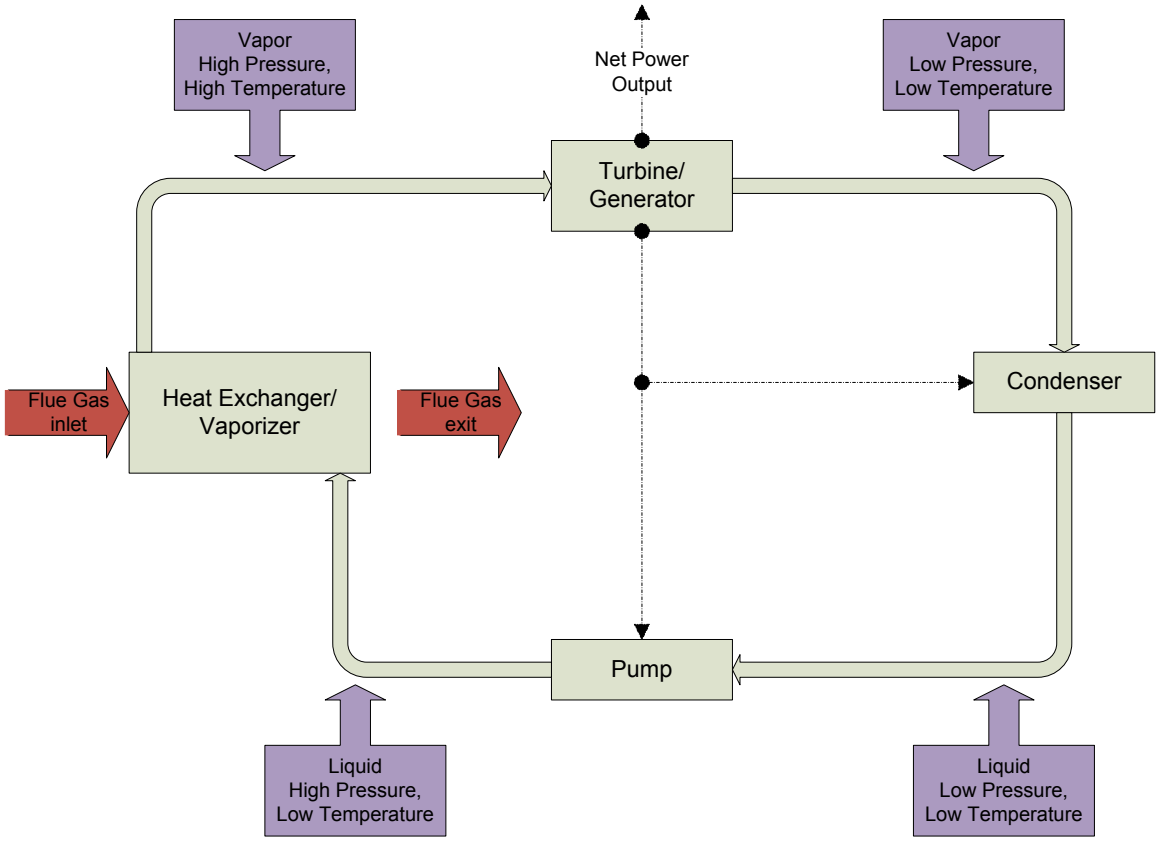

Figure 1 - Organic Rankine Cycle

In this study, the designs of heat exchangers/vaporizers for use in the ORC system are analyzed. Important heat exchanger dimensions such as tube diameter, transverse tube spacing and overall length are selected to minimize the pressure drops of flue gas and cooling fluid and overall cost.

2. THEORY

Heat exchangers can be used to condense the water & sulfuric acid present in flue gas. This type of heat exchanger is also called a condensing flue gas heat exchanger and it typically has flue gas and water as the two fluid streams.

Modeling the heat exchanger was done in MATLAB by previous ERC researchers. Jeong developed a code to simulate the heat transfer and condensation occurring inside the heat exchanger (3). The results from the code were validated with data obtained from an experimental study. Hazell (4) and Goel (5) further developed the code to calculate the pressure drop in flue gas and cooling water streams and estimate heat exchanger costs. In the present study, the author made modifications in the code to model the condensation of sulfuric acid present in flue gas.

A separate MATLAB code was also developed by the author for the heat exchanger used in the Organic Rankine Cycle. This code calculates the heat transfer between the flue gas and cooling fluid, R-245fa as well as pressure drop on both the flue gas side and cooling fluid side of the tube. This code also estimates the cost to install and operate the heat exchanger at a given facility.

2.1 Analytical modeling of Sulfuric Acid Condensation

Sulfuric acid condensation takes place when the tube wall temperature falls below the acid dew point. Flue gas coming out of an air pre-heater (APH) can have

concentrations of sulfuric acid up to 50 ppm. The dew point temperature of sulfuric acid depends on the mole fraction of the water vapor and acid in the flue gas. Different types of coals have different sulfur and moisture contents. In general, the dew point temperature of sulfuric acid in the flue gas ranges in between 230 to 315 ^{0}F (3). The dew point temperature of H_2SO_4 increases with increase in both water vapor and acid mole fractions in the flue gas. The variation of dew point temperature of sulfuric acid with inlet mole fraction of sulfuric acid and moisture in the flue gas is illustrated in figure 2.

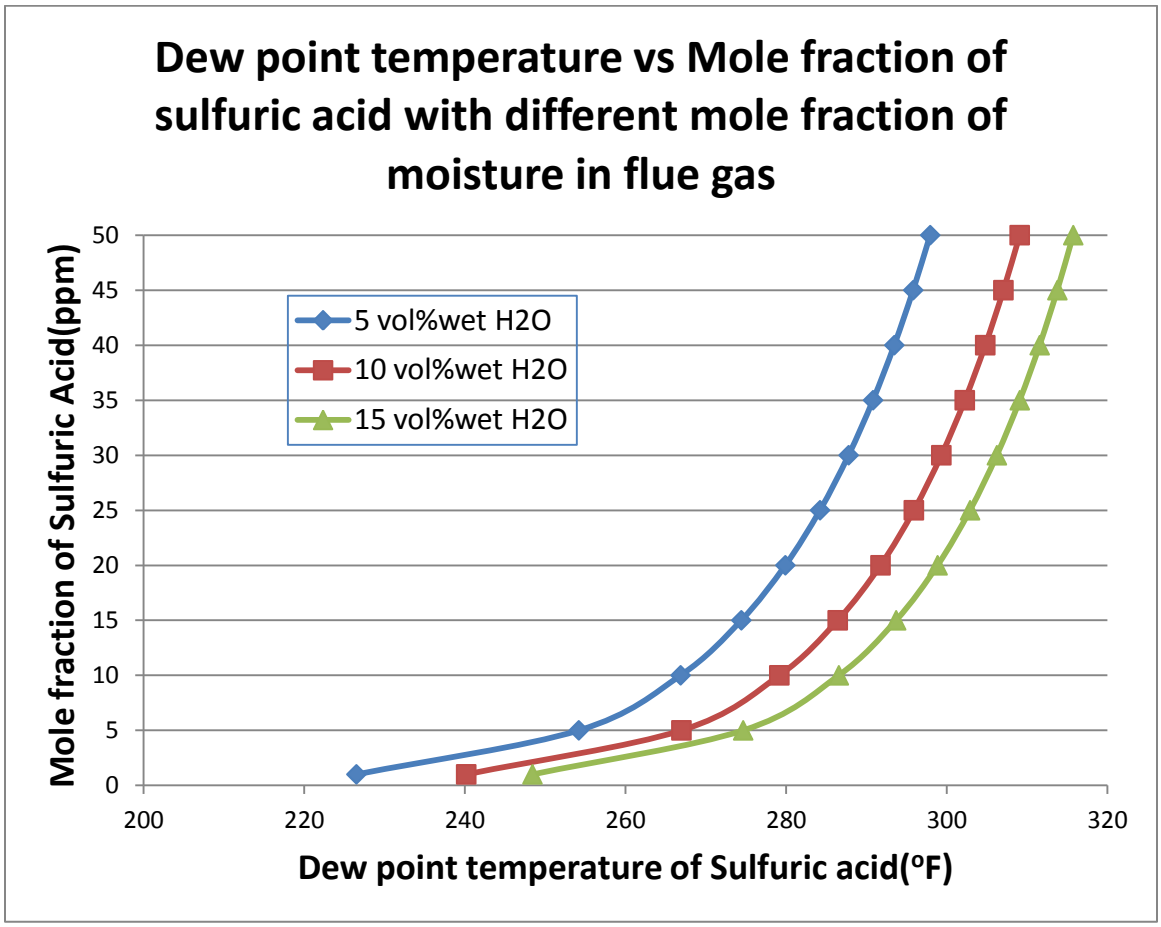

Figure 2 - Dew point temperature of sulfuric acid in the presence of non-condensable gas

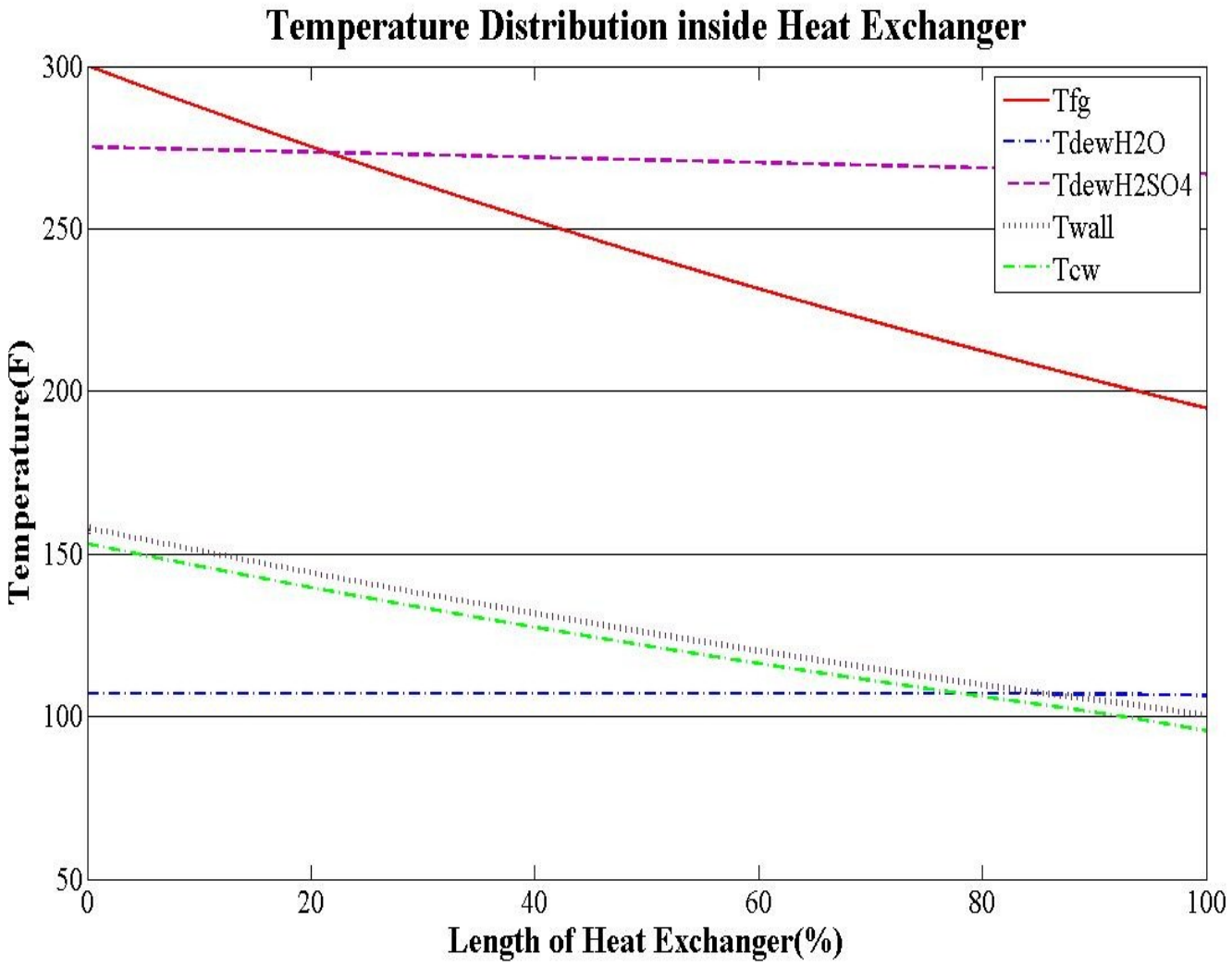

Figure 3 - Temperature profiles of important parameters inside a Heat Exchanger

Sulfuric acid condensation in the flue gas occurs in the presence of non-condensable gas components. Colburn and Hougen developed an equation for condensation in the presence of a non-condensable gas. When the temperature of tube wall through which the water flows falls below the dew point temperature of moisture in the flue gas, water condensation takes place. The Colburn-Hougen equation given below explains the phenomenon (6)

$$h_{fg}(T_{fg} - T_i) + k_m L_g(y_{H_2O} - y_i) = U_0(T_i - T_{cw}) \quad (2.1)$$

Where,

h_{fg}	-	Convective heat transfer coefficient
T_{fg}	-	Bulk temperature of flue gas
T_i	-	Gas-condensate film interfacial temperature
k_m	-	Mass transfer coefficient
L_g	-	Latent heat of Water Vapor
y_{H_2O}	-	Mole fraction of water vapor in flue gas
y_i	-	Mole fraction of water vapor at the gas-condensate interface
T_{cw}	-	Temperature of cooling water
U_0	-	Overall heat transfer coefficient

In the above equation, the first term on left hand side gives the sensible heat transfer from flue gas to the tube wall interface and second term gives the latent heat transfer due to condensation of moisture in the flue gas. The latent heat transfer due to condensation of sulfuric acid in the flue gas is neglected as its magnitude is very small when compared to the latent heat of water vapor.

U_0 in the above equation is the overall heat transfer coefficient given by:

$$\frac{1}{U_0 A_{eff}} = \left[\frac{1}{h_{cw}} + R_{fl}\right]\frac{1}{A_i} + R_{wall} + \frac{1}{h_f A_o} \quad (2.2)$$

Where,

A_{eff}	-	Effective area assumed to be equal to A_o
A_o	-	Outer surface area of tube
A_i	-	Inner surface area of tube
R_{fl}	-	Thermal resistance due to fouling on the inner-side of tube
R_{wall}	-	Thermal resistance of tube wall
h_{cw}	-	Convective heat transfer coefficient for cooling water
h_f	-	Convective heat transfer coefficient for condensate film formed on the outer surface of the tube

R_{wall} is a function of thermal conductivity of tube, overall length of tube as well as the inner and outer diameters.

$$R_{wall} = \frac{ln\left(d_o/d_i\right)}{2\pi k_w L} \tag{2.3}$$

Where,

d_o	-	Outer diameter of the tube
d_i	-	Inner diameter of the tube
L	-	Overall length of the tube
k_w	-	Thermal conductivity of the tube

Thermal resistance due to fouling is neglected as in most of the cases, the cooling fluid used is from a clean source. Also, the thermal resistance due to the condensate film can also be neglected because of negligible thickness. Substituting the surface area as the product of the circumference and the overall length of the tube, L, and solving for U_0, the equation (2.2) reduces to:

$$U_0 = \frac{1}{\frac{r_o}{r_i}\frac{1}{h_{cw}} + \frac{r_o}{k_w} ln\frac{r_o}{r_i}} \tag{2.4}$$

The expression for T_i can be formulated by substituting the value of U_o from equation (2.4) into equation (2.1):

$$T_i = \frac{\left[h_{fg}T_{fg} + \left(\frac{1}{\frac{r_o}{r_i}\frac{1}{h_{cw}} + \frac{r_o}{k_w} ln\frac{r_o}{r_i}}\right) * T_{cw} + k_m L_g\left(y_{H_2O} - y_i\right)\right]}{\left[\left(\frac{1}{\frac{r_o}{r_i}\frac{1}{h_{cw}} + \frac{r_o}{k_w} ln\frac{r_o}{r_i}}\right) + h_{fg}\right]} \tag{2.5}$$

When there is no condensation, the mass transfer term can be dropped from the equation (2.1). The rate of heat transfer reduces to a simple equation:

$$q = \frac{T_{fg} - T_{cw}}{R_{total}} \tag{2.6}$$

Where, R_{total} is given by:

$$R_{total} = R_{flue\ gas} + R_{wall} + R_{cooling\ water} \tag{2.7}$$

and,

$$R_{flue\ gas} = \frac{1}{h_{fg} A_o} = \frac{1}{2\pi r_o L h_{fg}} \tag{2.8}$$

$$R_{cooling\ water} = \frac{1}{h_{cw} A_i} = \frac{1}{2\pi r_i L h_{cw}} \tag{2.9}$$

Heat is transferred from flue gas to the cooling water through the tube wall. The heat exchanger is discretized into number of small cells and the heat balance equations are applied for each cell in order to calculate the exit flue gas and cooling water temperatures. The tube portion shown in Fig. 4 represents a discretized cell of the heat exchanger. The flue gas and cooling water flow directions are also shown:

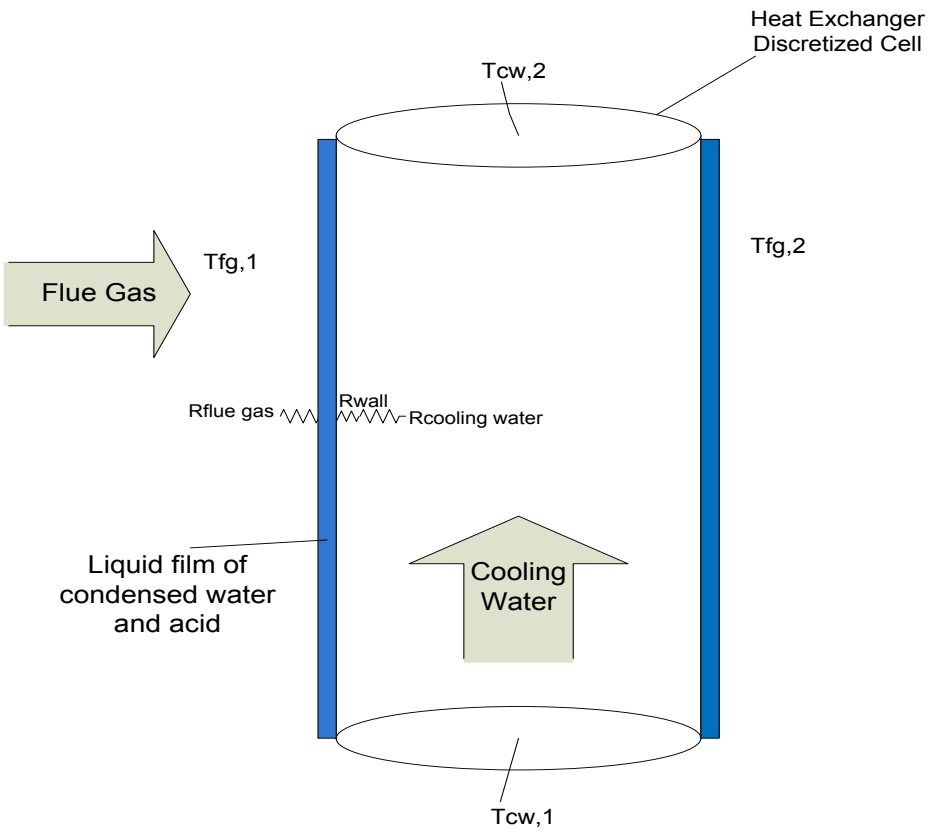

Figure 4 - Thermal Resistances between flue gas and cooling water

Assuming negligible condensation at the first discretized cell of the heat exchanger, the heat balance equation is given by:

$$q = h_{fg} A_{oc} \left(T_{fg} - T_{ow} \right) \tag{2.10}$$

Where,

A_{oc}	-	Outer wall surface area of cell
T_{fg}	-	Mean flue gas temperature in the first cell
T_{ow}	-	Outer wall temperature of cell
A_i	-	Inner surface area of tube

Rearranging the equation (2.10), an expression for initial outer tube wall temperature can be obtained:

$$T_{ow} = T_{fg} - \frac{q}{h_{fg} A_{oc}} \tag{2.11}$$

Applying the law of conservation of energy between the flue gas and the tube wall, the following expression can be obtained:

$$\dot{m}_{fg} C_{p,fg} \left(T_{fg,2} - T_{fg,1}\right) = h_{fg} \left(T_{fg} - T_{ow,1}\right) A_{oc} \tag{2.12}$$

Where,

T_{fg} - Average of the flue gas inlet and exit temperature for the cell.

The flue gas temperature at the exit of the new cell is calculated by using $T_{fg,2}$, $T_{cw,2}$, $T_{ow,2}$, $T_{iw,2}$ from the previous cell as the inlet conditions to the current cell. Rearranging the equation (2.12),

$$T_{fg,2} = \frac{\left(\dot{m}_{fg} C_{p,fg} - 0.5 * h_{fg} A_{oc}\right) * T_{fg,1} + h_{fg} A_{oc} T_{ow,1}}{\dot{m}_{fg} C_{p,fg} + 0.5 * h_{fg} A_{oc}} \tag{2.13}$$

Also, from the energy conservation law, it can be inferred that the total change in enthalpy of the cooling water should be equal to the total heat transferred to the wall from the flue gas. Thus for the current cell:

$$h_{fg} \left(T_{fg} - T_{ow,1}\right) A_{oc} = \dot{m}_{cw} C_{p,cw} \left(T_{cw,2} - T_{cw,1}\right) \tag{2.14}$$

Rearranging the equation (2.14),

$$T_{cw,2} = T_{cw,1} - \frac{h_{fg} (T_{fg} - T_{ow,1}) A_{oc}}{\dot{m}_{cw} C_{p,cw}} \tag{2.15}$$

When there is condensation, the above equation is modified using Colburn-Hougen relation and the wall temperature $T_{ow,1}$ is replaced by the temperature of the gas-condensate interface, $T_{i,1}$. Equations (2.13) and (2.15) can be rewritten as:

$$T_{fg,2} = \frac{(\dot{m}_{fg}C_{p,fg} - 0.5*h_{fg}A_{oc})*T_{fg,1} + h_{fg}A_{oc}T_{i,1}}{\dot{m}_{fg}C_{p,fg} + 0.5*h_{fg}A_{oc}} \quad (2.16)$$

$$T_{cw,2} = T_{cw,1} - \frac{[h_{fg}(T_{fg} - T_{i,1}) + k_m h_l (y_{H_2O} - y_i)]A_{oc}}{\dot{m}_{cw}C_{p,cw}} \quad (2.17)$$

The temperature of the inner wall is calculated by considering the enthalpy change in the cooling water as expressed below:

$$h_{cw}A_{ic}(T_{iw,2} - T_{cw,2}) = \dot{m}_{cw}C_{p,cw}(T_{cw,1} - T_{cw,2}) \quad (2.18)$$

Rearranging equation (2.18),

$$T_{iw,2} = T_{cw,2} + \frac{\dot{m}_{cw}C_{p,cw}(T_{cw,1} - T_{cw,2})}{h_{cw}A_{ic}} \quad (2.19)$$

The outer wall temperature at the cell exit is calculated from the same energy balance principle applied between the enthalpy change in cooling water and rate of heat transfer between the tube outer and inner wall.

$$q = \frac{(T_{ow,2} - T_{iw,2})}{R_{wall}} = \dot{m}_{cw}C_{p,cw}(T_{cw,2} - T_{cw,1}) \quad (2.20)$$

Substituting the expression for R_{wall} from equation (2.3) in the equation (2.20) and rearranging,

$$T_{ow,2} = T_{iw,2} + \frac{\dot{m}_{cw}C_{p,cw}(T_{cw,1} - T_{cw,2})\ln {}^{r_o}/_{r_i}}{2\pi k_w L} \quad (2.21)$$

It is necessary to calculate the water vapor mole fraction at the interface and convective heat transfer coefficients for flue gas and cooling water for the calculation of all the temperatures described in the equations above. All the thermodynamic properties described below are calculated at each discrete cell and then averaged over the entire tube length. For exchanger with bank of bare tubes in inline arrangement, an empirical relation to calculate the Nusselt number was proposed by Zukauskas (7).

$$Nu_{fg} = C.Re_{fg,max}^{m}.Pr^{0.36}.\left(\frac{Pr}{Pr_s}\right)^{1/4} \quad (2.22)$$

Where,

Nu_{fg}	-	Nusselt number of flue gas flow
Pr	-	Prandtl number
Pr_s	-	Surface Prandtl number
Re	-	Reynolds number

The variables C and m depend on the Reynolds number of flue gas flow. The value of C is around 0.27 if the maximum of Reynolds number ranges between 1000 and 20,000. The value of m is evaluated graphically based on experimental data from Zukauskas (7). The convective heat transfer coefficient for flue gas can be calculated as:

$$h_{fg} = \frac{Nu_{fg}k_{fg}}{d_o} \quad (2.23)$$

The Nusselt number for the cooling water flow is obtained from the expression given by Gnielinski (8)

$$Nu_{cw} = \frac{(f/8)(Re_{cw}-1000)Pr}{1+12.7(f/8)^{1/2}\left(Pr^{2/3}-1\right)} \quad (2.24)$$

If the Reynolds number of cooling water flow (Re_{cw}) ranges between 3,000 to 5,000,000, the friction factor f is calculated from the Moody Diagram by using the equation (2.25) (9),

$$f = (0.79.\ln(\mathrm{Re_{cw}}) - 1.64)^{-2} \quad (2.25)$$

The convective heat transfer coefficient for cooling water is calculated using the equation (2.26)

$$h_{cw} = \frac{Nu_{cw}k_{cw}}{d_i} \quad (2.26)$$

The mole fraction of water vapor at the tube wall interface (y_i) is evaluated at the beginning of each cell using the Antoine equation (10)

$$y_i = \frac{e^{\left(a-\frac{b}{T_i+c}\right)}}{P_{tot}} \quad (2.27)$$

Where, a = 16.262, b = 3799.89 and c = 226.35 and P_{tot} is the total pressure of flue gas.

Rate of condensation of sulfuric acid per unit area is proportional to the difference between mole fraction of sulfuric acid in the flue gas and mole fraction of sulfuric acid evaluated at interfacial temperature assuming phase equilibrium. It can be calculated by integrating the differential equation (2.29) given below (11),

$$d\dot{m}_{cd,H_2SO_4}/dA = k_{m,H_2SO_4}.\left(y_{H_2SO_4} - y_{i,H_2SO_4}\right) \quad (2.28)$$

Where,

$d\dot{m}_{cd,H_2SO_4}$	-	Rate of condensation of sulfuric acid
k_{m,H_2SO_4}	-	Mass transfer coefficient of sulfuric acid
$y_{H_2SO_4}$	-	Mole fraction of sulfuric acid in the flue gas
y_{i,H_2SO_4}	-	Mole fraction of sulfuric acid at the interface
dA	-	Surface area of the cell

Mass transfer coefficient for sulfuric acid condensation is given by equation (2.29) below (12):

$$k_{m,H_2SO_4} = \frac{h_{fg}.M_{H_2SO_4}}{C_{p,fg}.M_g.y_{lm}.Le_{H_2SO_4-gas}^{2/3}} \quad (2.29)$$

Where,

h_{fg}	-	Convective heat transfer coefficient of flue gas
$M_{H_2SO_4}$	-	Molecular weight of sulfuric acid
M_g	-	Molecular weight of wet flue gas
y_{lm}	-	Logarithmic mean mole fraction of non-condensable gas between flue gas and the wall given by equation (2.28)

$$y_{lm} = \frac{y_{ni}-y_{nb}}{ln(y_{ni}-y_{nb})} \quad (2.30)$$

Where,

y_{ni}	-	Mole fraction of non-condensable gas in the bulk
y_{nb}	-	Mole fraction of non-condensable gas at the interface

The parameter $Le_{H_2SO_4-gas}$ is the Lewis number of sulfuric acid in the presence of flue gas. It is calculated by the equation (2.31) below:

$$Le_{H_2SO_4-gas} = \frac{Sc}{Pr} = \frac{\alpha_g}{D_{H_2SO_4-gas}} \quad (2.31)$$

Where,

Sc	-	Schmidt number

α_g - Thermal diffusivity of flue gas
$D_{H_2SO_4-gas}$ - Mass diffusivity of sulfuric acid in flue gas

The Lewis number of sulfuric acid in the flue gas is assumed to be approximately same as Lewis number of sulfuric acid in air.

$$Le_{H_2SO_4-gas} = Le_{H_2SO_4-air} \tag{2.32}$$

The mass diffusivity of sulfuric acid in the flue gas is calculated by the equation (2.33) derived from equation (2.32),

$$D_{H_2SO_4-gas} = D_{H_2SO_4-air} \cdot \frac{\alpha_g}{\alpha_{air}} \tag{2.33}$$

Where,

α_{air} - Thermal diffusivity of air
$D_{H_2SO_4-air}$ - Mass diffusivity of sulfuric acid in air given by the equation (2.34) below (13)

$$D_{H_2SO_4-air} = 5.0032 \times 10^{-6} + 1.04 \times 10^{-8}.\mathrm{T_{fg,K}} + 1.64 \times 10^{-11}.\mathrm{T^2_{fg,K}} - 1.566 \times 10^{-14}.\mathrm{T^3_{fg,K}} \tag{2.34}$$

Where,

$\mathrm{T_{fg,K}}$ - Mean temperature of flue gas in Kelvin

The equation used to calculate the interface mole fraction of sulfuric acid is given below (12):

$$y_{i,H_2SO_4} = \exp\left[\frac{\frac{1}{\mathrm{T_{i,K}}} - 0.002276 + 0.00002943.\ln(\mathrm{P_{i,H_2O}})}{6.20\times10^{-6}.\ln(\mathrm{P_{i,H_2O}}) - 0.0000858}\right] / \mathrm{P_{tot}} \tag{2.35}$$

Where,

$T_{i,K}$	-	Interfacial Temperature in Kelvin
P_{i,H_2O}	-	Partial pressure of water vapor at the interface in mmHg
P_{tot}	-	Total pressure at interface in mmHg

2.2 Organic Rankine Cycle (ORC) Heat Exchanger

The design of the heat exchanger used in the organic rankine cycle system is similar to the condensing heat exchanger described in 2.1. Flue gas is the high temperature fluid in both the cases but the low temperature fluid is different. In the case of condensing heat exchanger, water is the cooling fluid used and there is no water evaporation inside the tube bank. Working fluids such as refrigerants are used as cooling fluid in ORC heat exchanger which will be evaporated and superheated in the tube bank of heat exchanger.

The boiling temperature of organic refrigerants is low when compared to that of water. The refrigerant flowing through the heat exchanger tubes may start evaporating at a particular point when its temperature reaches saturation point at the given pressure.

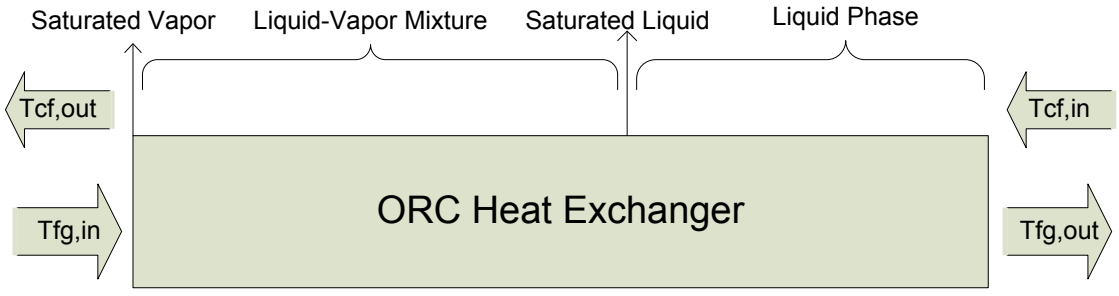

Figure 5 - ORC Heat Exchanger Model

Similar to the condensing heat exchanger, the ORC heat exchanger is also a counter flow heat exchanger. As shown in Fig. 5, the flue gas enters the heat exchanger from one side and the cooling fluid enters in a liquid state from the other side. When the temperature of cooling fluid reaches the saturation temperature, it starts evaporating and the heat energy transferred from flue gas is utilized by the cooling fluid as the latent heat of vaporization.

2.2.1 Assumptions and Simplifications

Analytical modeling in this study was developed with the following assumptions.

- The flows are one dimensional.
- Steady state is assumed.
- Two phases (gases and liquids) are assumed for both flue gas side and cooling fluid side
- Cooling fluid enters the heat exchanger as a sub cooled liquid exits the heat exchanger as a saturated vapor. No scope for super heating of vapor.
- The thermal resistance due to the liquid film is negligible in the liquid-vapor mixture region of cooling fluid. Thus interfacial temperature is same as wall temperature.
- The thermal resistance due to the tube wall is neglected when the cooling fluid is in a liquid-vapor two phase mixture.
- The temperature of cooling fluid is constant and equal to the saturation temperature when it is a two phase mixture.
- The heat and mass transfer phenomenon is similar to the condensation heat exchanger when the cooling fluid is in liquid phase.
- There is no evaporation of water vapor or sulfuric acid on the flue gas side.

- There is no heat loss through the duct wall of the condensing heat exchanger.
- There are no chemical reactions.

2.2.2 Energy Balance Equations

Total heat transfer from the flue gas is equal to the sum of latent heat of vaporization and rise in enthalpy of cooling fluid when it is in liquid phase. The Colburn-Hougen equation when the fluid is in the mixture phase is:

$$h_{fg}\left(T_{fg} - T_i\right) + k_m L_g\left(y_{H_2O} - y_i\right) = \dot{m}_{cf}.\, i_{c,fg}.\frac{dX}{dz} \tag{2.36}$$

Where,

$\dot{m}_{cf}$	-	Mass flow rate of cooling fluid
$i_{c,fg}$	-	Latent heat of cooling fluid
X	-	Quality of cooling fluid
Z	-	Length of heat exchanger

Equation (2.36) is applicable only when the cooling fluid is in the liquid-vapor mixture phase. When the heat exchanger is discretized into infinitesimal cells, the above equation for each cell will be:

$$X_{cf,in} = X_{cf,out} - \frac{\left[h_{fg}\left(T_{fg} - T_i\right) + k_m L_g\left(y_{H_2O} - y_i\right)\right] A_{oc}}{\dot{m}_{cf} i_{c,fg}} \tag{2.37}$$

From the assumptions, it is clear that the exit quality of cooling fluid in the first cell is equal to 1 as the state of cooling fluid in the first cell is saturated vapor. The calculations of other parameters in the above equation are similar to the condensation heat exchanger. Thus the quality of cooling fluid at each cell is evaluated.

When the inlet quality of cooling fluid in a particular cell becomes zero, it signifies the point of saturated liquid in the heat exchanger. From that point, the heat and mass transfer phenomenon is similar to the phenomenon in condensation heat exchanger.

2.2.3 Pressure Drop

There can be significant pressure drops when the two fluids, flue gas and cooling fluid pass along the heat exchanger. An ID fan is used to overcome the pressure drop on flue gas side and fluid circulation pump is required on cooling fluid side. Additional power is required to maintain these units. The flow is assumed to be turbulent throughout the heat exchanger on both flue gas side and cooling fluid side.

Pressure drop on flue gas side for a heat exchanger with tubes in an inline arrangement is determined by using the relation developed by Zukauskas. According to Zukauskas' relation, pressure drop is a function of the longitudinal and transverse Pitch, number of tube rows and the maximum Reynolds number of the flue gas flow (7) :

$$\Delta p_{fg} = N_L \chi \left(\frac{\rho_{fg} V_{max}^2}{2}\right) f \tag{2.38}$$

Where,

N_L	-	Number of rows
χ	-	Correction factor
ρ_{fg}	-	Density of flue gas
V_{max}	-	Maximum velocity between the tubes
f	-	Friction factor

The correction factor χ depends on the tube longitudinal and transverse pitch. The density, velocity and friction factor are calculated for each cell and the mean is calculated for the entire heat exchanger. The ID fan is assumed as an isentropic compressor and the

additional power required is obtained from the pressure drop by using simple thermodynamic equation:

$$Fan\ Power = \frac{\dot{m_{fg}} C_{p,fg}\left[\left(\frac{P_{out}}{P_{in}}\right)^{\frac{\gamma-1}{\gamma}} - 1\right]}{\eta_{fan}} \quad (2.39)$$

Where,

P_{in}	-	Atmospheric pressure, P_{atm}
P_{out}	-	$P_{atm} + \Delta p_{fg}$,
γ	-	$C_{p,g}/C_{v,g}$,
η_{fan}	-	Efficiency of the fan.

On the cooling fluid side, the vaporized fluid in the tube bank is removed at particular points in the heat exchanger. Thus, the mass flow rate of working fluid is decreased. In the pressure drop calculations, it was assumed that the mass flow rate of working fluid remains constant and it will be in liquid state. Darcy-Weisbach equation is used to calculate the pressure drop through the length of the tube which accounts for the major value of pressure drop magnitude (14)

$$\Delta p_l = f \frac{L}{d_i} \frac{\rho_{cw} V_{avg}^2}{2} \quad (2.40)$$

Where,

Δp_l	-	Pressure loss along the length of the tube,
f	-	Friction factor obtained from the Moody Diagram (9),
L	-	Total length of the tube,
ρ_{cw}	-	Density of cooling water and
d_i	-	Inner diameter of the tube.

Apart from the above head loss, minor pressure losses are also observed in the inlet and the outlet header, in the 180° elbows and due to sudden contraction and expansion of the cooling fluid. The cooling fluid pressure drop equations and calculations

are emphasized in detail in Hazell's thesis (4). The total pump power required to pump the cooling fluid through the tubes can then be calculated from the total pressure drop as:

$$Pump\ Power = \frac{Q\Delta p_{total}}{\eta_{pump}}$$

(2.41)

Where,

Q	-	Total Volume flow rate of cooling water
Δp_{total}	-	Total cooling fluid pressure drop
η_{pump}	-	Pump efficiency

2.3 Cost Calculation

The installation of heat exchanger involves the design and manufacture of the components and final assembly of the components. Also, the required dimensions of heat exchanger depend on the working conditions. It is essential to consider the economics of heat exchanger and obtain an optimized design of heat exchanger by maximizing the net heat recovery and minimizing cost. The economics of heat exchanger are explained in detail in Hazell's work (4). There are two types of costs associated with heat exchanger. They are: fixed cost and operating cost.

2.3.1 Fixed Cost

The fixed cost, also known as capital cost, comprises the cost of material and the manufacturing and installation cost for the duct and the tubes. The fixed cost of condensing heat exchangers is mainly the tube material cost and its installation. In studies done on cost estimation of shell and tube heat exchangers (15), it was observed that the

cost of tube material increases with size while the fabrication and assembly costs proportionally decrease with size.

The type of tube material used for the tubes is one of the major factors that affect the total cost. In general, carbon steel tubes are inexpensive but they have more tendencies to get corroded due to acid and water vapor condensation. Nickel alloy 22 tubes are used in the portion of condensing heat exchanger where acid condensation is high and stainless steel SS304 is used thereafter. Nickel alloy 22 material is very expensive compared to SS304 and carbon steel. It is assumed that the manufacturing and installation costs are same irrespective of the tube material type. The choice of materials is based on the detailed study done by Hazell (4). Assuming negligible price inflation since his study, the same pricing of $14.89/ft for manufacturing and installation cost any tube material with dimensions 2" diameter NPS and 0.195" thickness has been used. The cost of material for SS304 tubes was assumed to be $10.69/ft, $110.71/ft for Nickel alloy 22 tubes and $3.82/ft for carbon steel tubes of previously mentioned dimensions. Also, the quotes for above tube materials from various suppliers can be found in Hazell's thesis in detail.

The loan period and life expectancy of Heat exchanger was assumed to be 20 years and an annual rate of interest of 5%, a monthly payment factor was calculated using the equation (2.42) (16):

$$PF = \frac{i(1+i)^n}{(1+i)^n - 1} \tag{2.42}$$

Where,

PF	-	Monthly payment factor,
i	-	Monthly rate of interest
n	-	Total period of loan in months= 12 x 20

The annual fixed cost of the heat exchanger can then be calculated from the total fixed cost as:

$$AFC = (12 * PF + TIF) * (Total\ Fixed\ Cost) \quad (2.43)$$

Where,

AFC	-	Annual fixed cost
TIF	-	Taxes and insurance factor, assumed to be 0.015

2.3.2 Operating Cost

Heat exchanger requires external devices such as ID fan and cooling fluid circulating pump in order to assist both the flue gas flow as well as cooling fluid flow. The power requirements to operate ID fan and pump can be calculated from the pressure drop also explained in the section 2.3.3. Assuming that the heat exchanger will remain in service for 7000 hours per year and the cost of electricity is $60/MWhr, the annual operating cost is given as:

$$AOC = Power\ (in\ MW) * \frac{7000\ hrs}{year} * {\$60}/{MWhr} \quad (2.44)$$

Where,

AOC	-	Annual Operating Cost
Power	-	$Fan\ Power + Pump\ Power$.

3. SULFURIC ACID CONDENSATION RESULTS

As mentioned earlier, the MATLAB code developed by previous researchers has been modified to analyze the sulfuric acid condensation also, apart from water vapor condensation in the full scale heat exchanger. The modified code was used to predict the condensation rates of sulfuric acid in three different cases. The working conditions as well as the coal used were different in the cases analyzed. The table below gives the working conditions and other factors in detail.

Table 1 - Sulfuric acid condensation test cases

		Case – 1	Case – 2	Case – 3
Type of Coal	**-**	PRB Coal	Bituminous Coal	N.D. Lignite
T_{fg} in	**^{o}F**	300	300	300
T_{cw} in	**^{o}F**	90	90	90
M_{FG}	**[10^6 lb/hr]**	6.3	6.3	6.3
M_{CW}/ M_{FG}	**-**	0.5	0.5	0.5
y_{H2O}	**vol%wet**	12	8	15.9
y_{H2SO4}	**ppm**	1, 3 & 5	1, 5, 10, 20 & 30	1, 5 & 10

Where,

T_{fg} in	-	Inlet flue gas temperature
T_{cw} in	-	Inlet cooling water temperature
M_{FG}	-	Flue gas flow rate
M_{CW}	-	Cooling water flow rate
y_{H2O}	-	Mole fraction of moisture in flue gas at inlet
y_{H2SO4}	-	Mole fraction of Sulfuric acid in flue gas at inlet

Each case is again assumed to have different values of sulfuric acid present in the flue gas at heat exchanger inlet. For these analyses of heat exchangers, tube nominal pipe

size (NPS) pipe was kept constant at 2" and tube wall thickness was assumed to be 0.195". The tube spacings of S_t = 6.17" and S_l = 2.97" were used based on the optimization analysis done by Hazell (4). The geometry of heat exchanger used is summarized in Table – 2 below.

Table 2 - Heat Exchanger Geometry used in Sulfuric acid condensation tests

Tube NPS (in)	Tube Wall Thickness (in)	S_t (in)	S_l (in)	Duct Depth (ft)	Duct Height (ft)	Duct Length (ft)
2	0.195	6.17	2.97	40	40	20

3.1 Case -1: PRB Coal

In this case, the type of coal used is Powder River Basin (PRB) coal. Three subcases were studied. Each subcase has different sulfuric acid mole fractions in the flue gas at inlet. The subcases analyzed were assumed to have inlet mole fractions of 1, 3 & 5 ppm. The rest of the working conditions are same in all the three subcases.

The distribution of temperatures of various attributes over the length of heat exchanger is shown in the Fig. 6. The temperature distribution is similar for all the three subcases as all the inputs remain same except the inlet mole fractions of sulfuric acid and water vapor in the flue gas. Fig.7 shows how the mole fraction of sulfuric acid in flue gas varies throughout the length of heat exchanger in all the three subcases. The trends for rate of condensation of acid per unit area over the length of exchanger in all the three sub cases are given in Fig. 8.

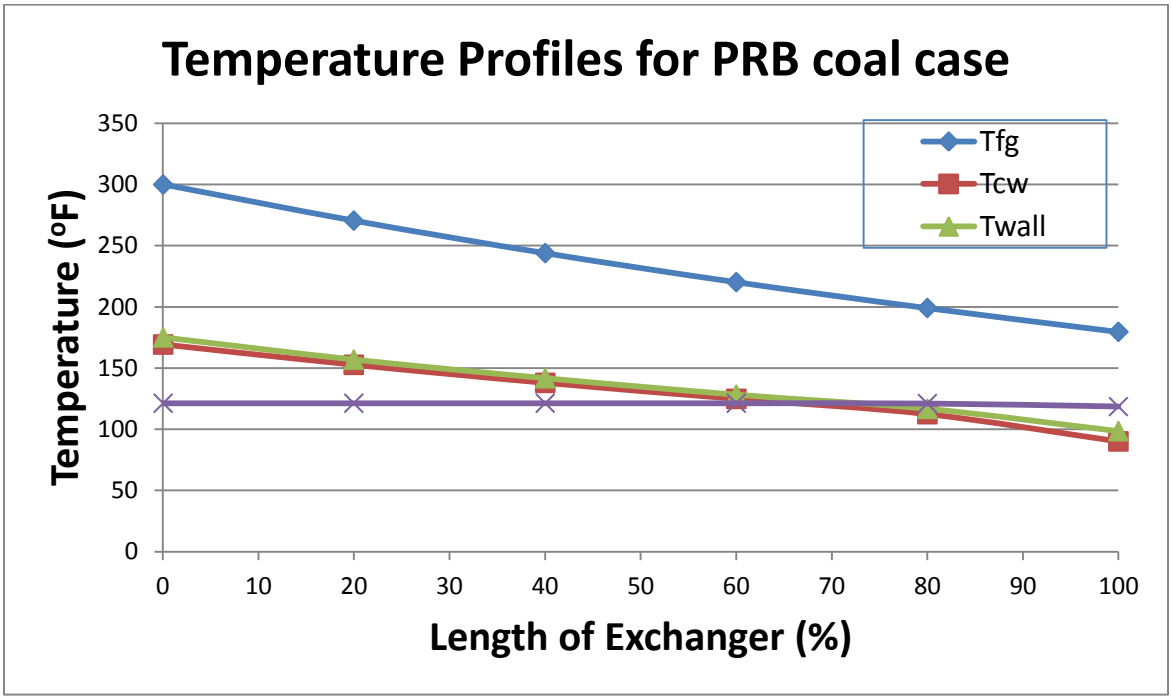

Figure 6 - Temperature profiles for PRB coal case

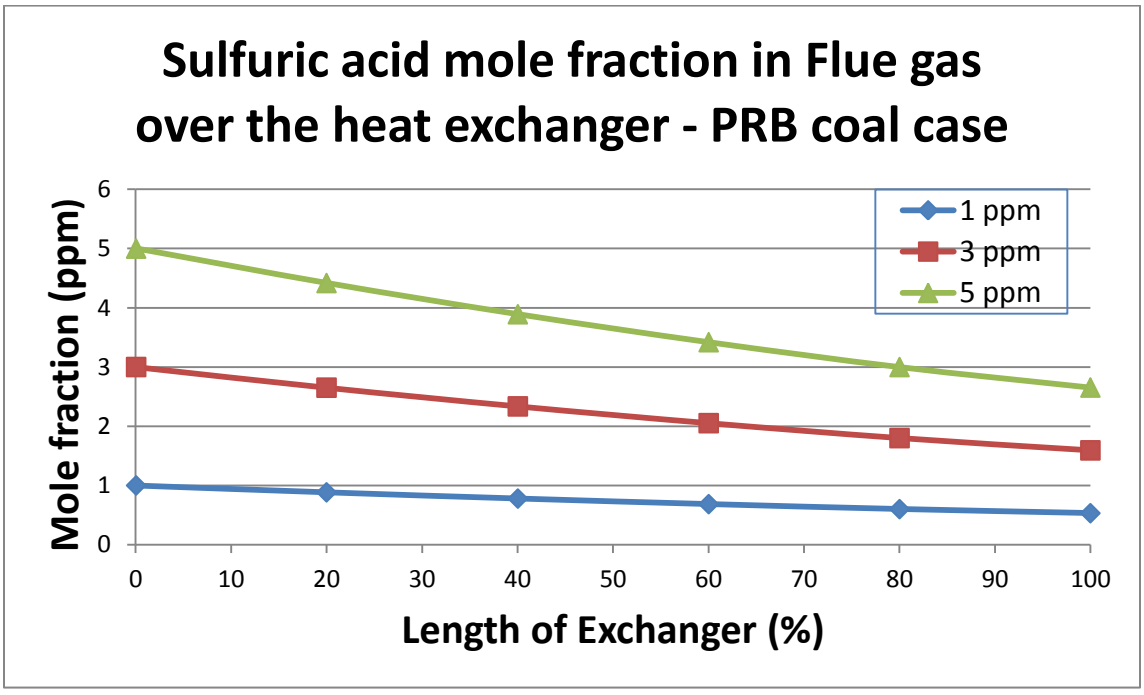

Figure 7 - Variation of mole fraction of sulfuric acid in Flue gas - PRB coal case

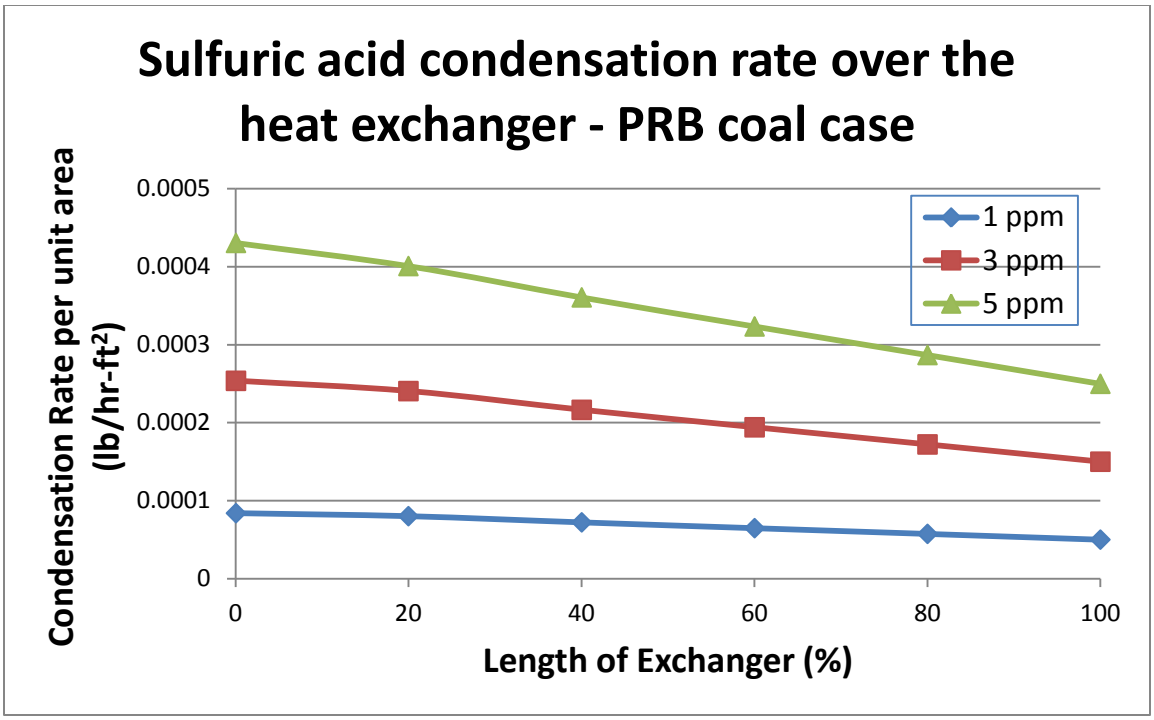

Figure 8 - Trend for rate of condensation of sulfuric acid over the length of heat exchanger – PRB coal case

3.2 Case -2: Bituminous coal

The type of coal used in this case was bituminous coal. Five subcases were studied. The subcases analyzed were assumed to have inlet mole fractions of 1, 5, 10, 20 & 30 ppm. Similar to the PRB coal case, the rest of the working conditions are same in all the subcases.

Figures below are the plots of temperature profile, sulfuric acid condensation rate and sulfuric acid mole fraction in flue gas over the length of heat exchanger.

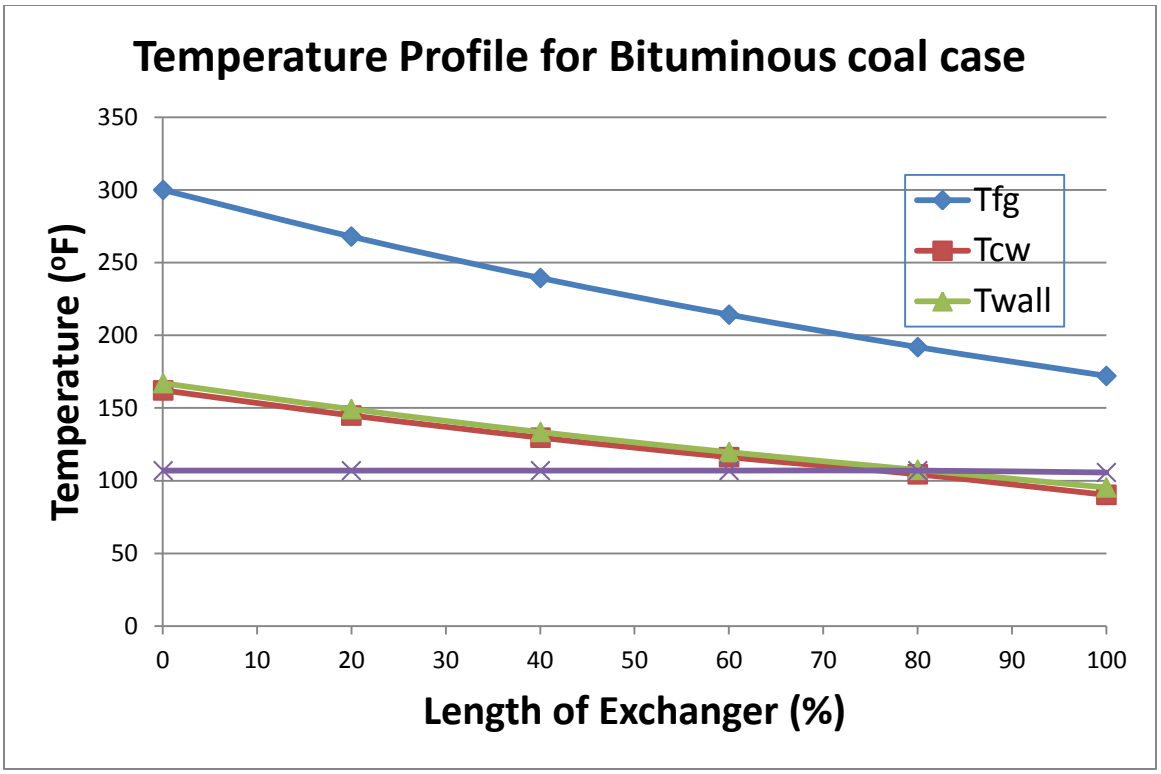

Figure 9 - Temperature profile for Bituminous coal case

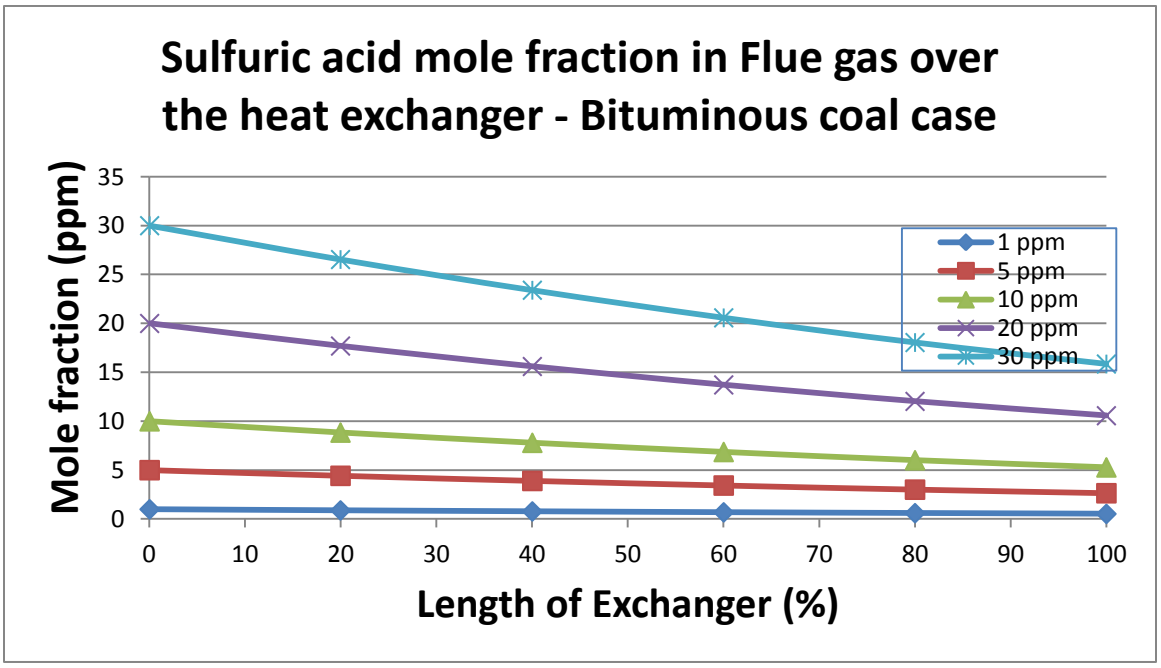

Figure 10 - Variation of mole fraction of sulfuric acid in Flue gas - Bituminous coal Case

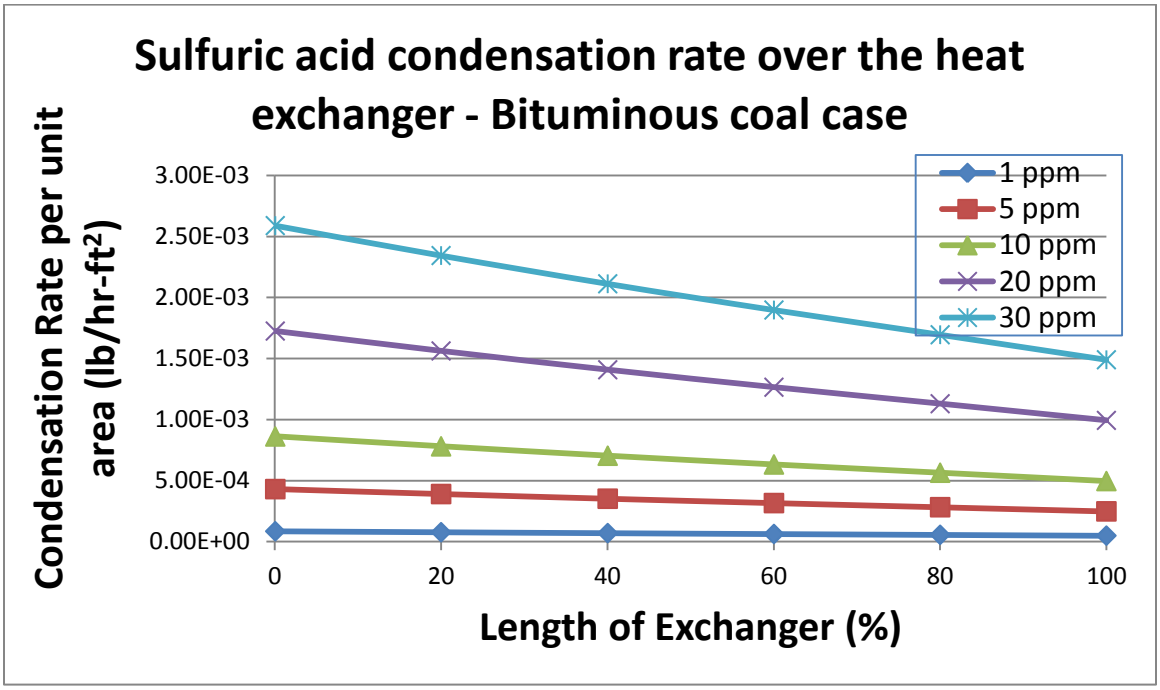

Figure 11 - Trend for rate of condensation of sulfuric acid over the length of heat exchanger – Bituminous coal case

3.3 Case -3: N.D. Lignite

The type of coal used in this case was North Dakota (N.D) lignite. Three subcases were studied. The subcases analyzed were assumed to have inlet mole fractions of 1, 5 & 10 ppm. See table 1 for the heat exchanger process conditions.

Figures below are the plots of temperature profile, sulfuric acid condensation rate and sulfuric acid mole fraction in flue gas over the length of heat exchanger.

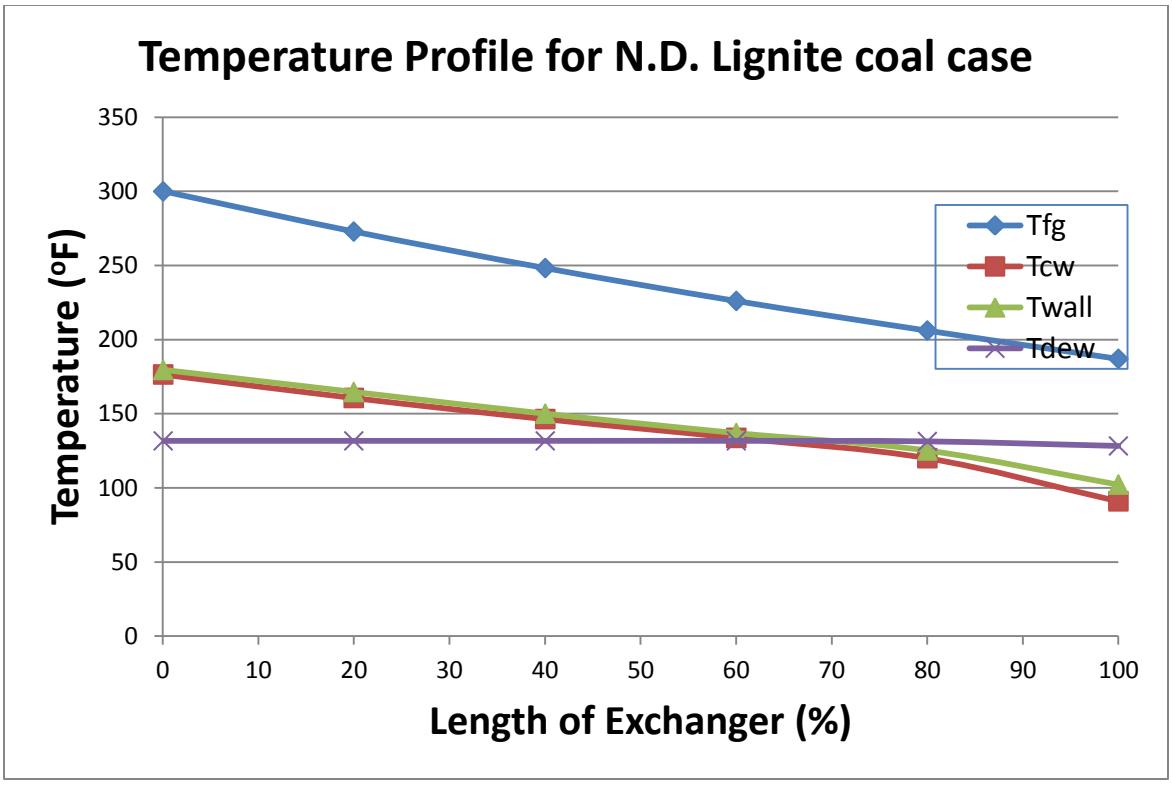

Figure 12 - Temperature profile for N.D. Lignite coal case

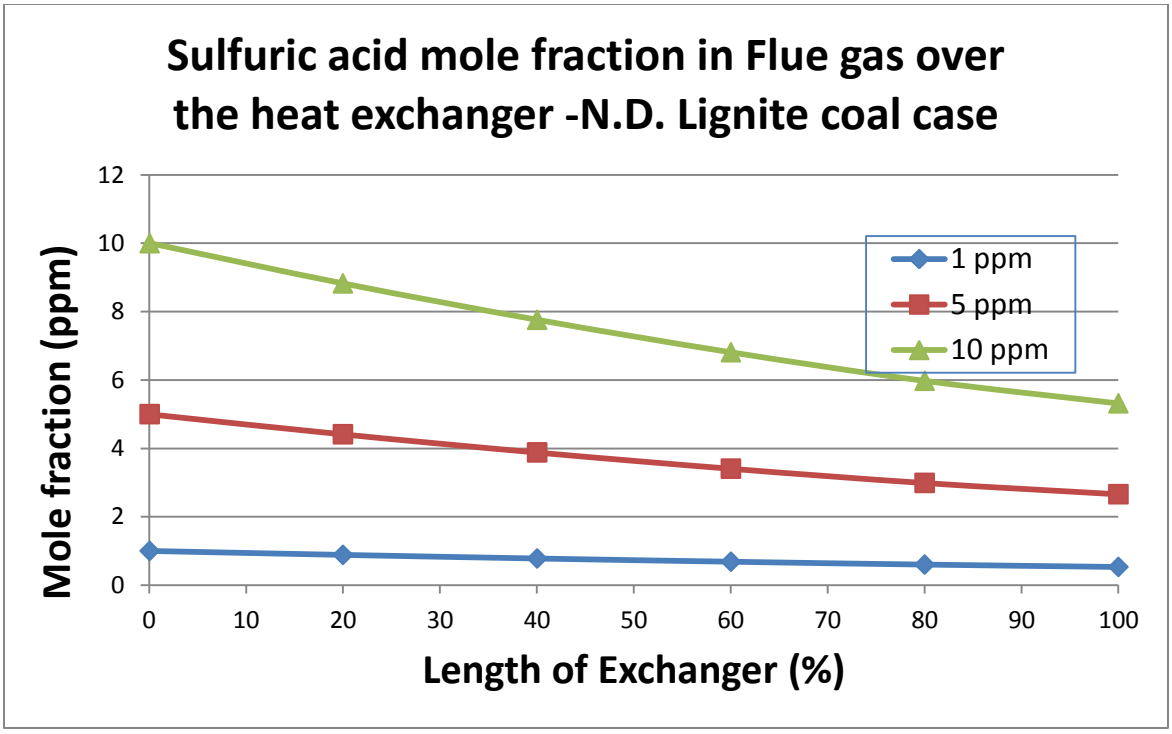

Figure 13 - Variation of mole fraction of sulfuric acid in Flue gas – N.D. Lignite coal case

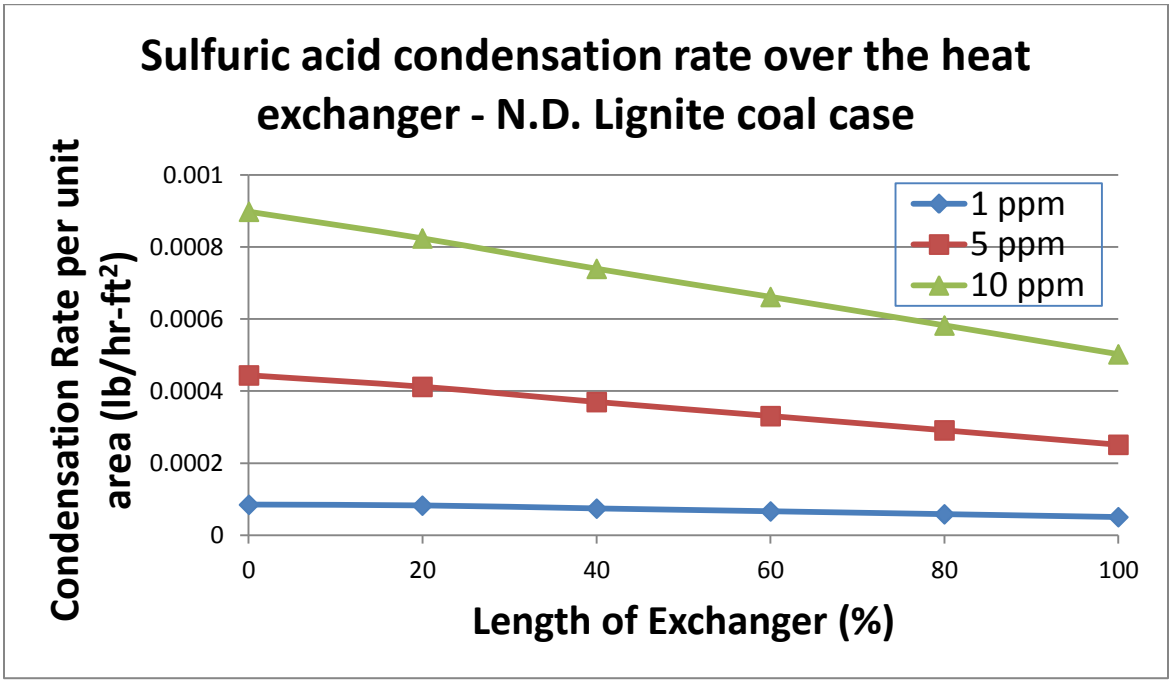

Figure 14 - Trend for rate of condensation of sulfuric acid over the length of heat exchanger – N.D. Lignite coal case

From the above temperature profile plots in all the three cases, it is clear that the temperatures of flue gas, cooling water and tube wall decrease as we proceed towards the flue gas exit end of heat exchanger. Also, the difference between the temperatures of tube wall and cooling water increases when the moisture in the flue gas condenses on the tube wall. This is due to the release of latent heat of condensation of water.

It is evident from the above plots that the sulfuric acid mole fraction present in the flue gas decreases as we move away from the inlet. Thus, the rate of condensation of sulfuric acid decreases due to decrease in the mole fraction of sulfuric acid in the flue gas.

The magnitudes of rates of condensation of sulfuric acid per unit area at selected points of heat exchanger are shown in table 3. The condensation rates for all the three cases given in the table are calculated assuming the inlet mole fraction of sulfuric acid in the flue gas are 5 ppm and the flue gas flow rate is $6.3x10^6$ lbm/hr. The mole fraction of water vapor in the flue gas is the main factor that affects the condensation rate of sulfuric acid for the given inlet conditions. N.D lignite coal case has the highest moisture content (15.9%) in flue gas, PRB coal has 12% and bituminous coal has lowest moisture content (8%). It can be noticed from the table that the sulfuric acid condensation rate is highest for N.D lignite coal and lowest for bituminous coal. Thus, it is evident that condensation of sulfuric acid is proportional to the fraction of moisture in the flue gas. The difference between sulfuric acid condensation rates in any two cases decreases as we proceed towards the flue gas exit side of heat exchanger. For example, the difference between condensation rates per unit area in PRB coal and N.D. lignite cases is 0.12×10^{-4} near the flue gas inlet of heat exchanger and 0.02×10^{-4} near the flue gas exit. The reason behind this notable difference is the decrement in mole fraction of water vapor in flue gas due to water condensation.

Table 3 - Rate of acid condensation per unit area at selected points of heat exchanger for all the three test cases when flue gas flow rate is 6.3×10^6 lbm/hr & inlet mole fraction of sulfuric acid in the flue gas is 5 ppm

	Length of heat exchanger (in %)						
Rate of condensation per unit area ($\times 10^{-4}$ lb/hr-ft^2)	**Coal Type**	Inlet (0%)	20%	40%	60%	80%	Exit (100%)
	PRB Coal	4.43	4.01	3.61	3.23	2.87	2.5
	Bituminous	4.31	3.90	3.52	3.16	2.83	2.48
	Lignite	4.56	4.12	3.70	3.31	2.91	2.51

4. SIMULATION RESULTS OF HEAT EXCHANGER USED IN ORGANIC RANKINE CYCLE

The analysis of heat exchanger which functions as evaporator of liquid refrigerant (also called as working fluid) in ORC was done by using the MATLAB code developed by the author. Simulations were performed for 3 test cases which have different working conditions. The properties of working fluid used in the simulations are based on physical properties of refrigerant R-245fa (1,1,1,3,3 - pentafluoropropane). The working fluid is assumed to be in the saturated vapor state at the exit of heat exchanger. Major details of working conditions are provided in the table below.

Table 4 - Working conditions of ORC evaporator simulations

	Units	Case – 1	Case – 2	Case – 3
Fuel type	-	Natural gas	Pulverized coal	Natural gas
T_{fg} in	^{o}F	189	313	216
T_{cf} in	^{o}F	93	80	96
M_{FG}	[lbm/hr]	3,360,000	6,736,000	3,353,000
M_{CF}	[lbm/hr]	595,123	2,955,730	814,153
y_{H2O}	vol%wet	10	10	10
P_{cf}	psia	63.75	189.5	74.25

Where,

T_{fg} in - Inlet flue gas temperature
T_{cf} in - Inlet working fluid temperature
M_{FG} - Flue gas flow rate
M_{CF} - Working fluid flow rate
y_{H2O} - Mole fraction of moisture in flue gas at inlet
P_{cf} - Working fluid pressure in the evaporator (heat exchanger)

The three ORC cases analyzed are: 1. Power plant based on natural gas combined cycle (NGCC), 2. Power plant using pulverized coal and 3. Power plant based on natural gas combined cycle with cogeneration (NGCC Cogeneration).

The mole fraction of moisture in flue gas is assumed to be 10% vol. wet in all the three cases. The change in pressure of the working fluid is assumed to be relatively small throughout the heat exchanger and thus the latent heat of vaporization of working fluid is constant. Simulation results include flue gas and working fluid parameters like total change in enthalpy etc., pressure drop calculations on both the flue gas side and working fluid side and cost calculations. Further details of working conditions which include the heat exchanger dimensions and simulation results are given in the following sub chapters.

4.1 Natural gas combined cycle (NGCC) case

In this case, the source of flue gas used in organic rankine cycle is natural gas. Simulations are performed for two heat exchangers (2 subcases of NGCC) which differ in the transverse spacing (S_t) of tubes in the heat exchanger. The parameter, S_t affects the overall length of heat exchanger, pressure drop and thus the cost pertaining to installation and maintenance of heat exchanger. The working conditions of the NGCC case simulation are given in table 5. These are same for both the subcases. Table 6 contains the information on heat exchanger dimensions used in the simulation for the two subcases.

Table 5 - Working conditions (inputs) for NGCC

	Units	Magnitude
Flue gas inlet temperature	^{o}F	189
Flue gas flow rate	lbm/hr	3,360,000
Working fluid inlet temperature	^{o}F	93
Working fluid flow Rate	lbm/hr	595,123
Working fluid to flue gas flow rate ratio	-	0.1771
Working fluid inlet pressure	psia	63.75
Working fluid exit temperature (saturated vapor)	^{o}F	136.58
Inlet mole fraction of water vapor in flue gas	-	0.10

Table 6 - Design data of heat exchangers used in NGCC case

	Units	Sub case -1	Sub case -2
Duct height	ft	40	40
Duct depth	ft	40	40
Duct length	ft	50.99	35.33
Tube outer diameter	in	2.375	2.375
Transverse spacing, S_t	in	**6.17**	**4.75**
Longitudinal spacing, S_l	in	2.97	2.97
Total surface area of tube bank	ft^2	382,000	349,250

From table 6, it can be noticed that the required total length of heat exchanger decreased as the transverse spacing, S_t is reduced. With less transverse spacing, more heat can be transferred from flue gas to working fluid for the given length. Thus, the required surface area of tube bank also reduces with S_t. From table 7, it can be observed that the point of condensation of water shifts towards the flue gas exit end of heat exchanger if S_t is lowered.

Table 7 - Flue gas parameters calculated in NGCC case

	Units	Sub case -1	Sub case -2
Exit flue gas (FG) temperature calculated	^{o}F	133.5	133.14
Sensible heat transfer rate from FG	Btu/hr	$4.96x\ 10^7$	4.99×10^7
Latent heat transfer rate from FG due to moisture condensation	Btu/hr	0.23×10^7	$0.2x\ 10^7$
Total heat transfer rate from FG	Btu/hr	5.19×10^7	$5.19x\ 10^7$
H_2O condensation start point (in % of total length)	-	98.17	97.92
Calculated heat exchanger duct length	ft	50.99	35.33
H_2O condensation start point, L[ft] (as 0< L< Duct Length)	ft	50.06	34.60

Table 8 - Working Fluid parameters calculated in NGCC case

	Units	Sub case -1	Sub case -2
Working fluid rate of enthalpy change from inlet saturated liquid state	Btu/hr	0.86×10^7	$0.86x\ 10^7$
Working fluid rate of enthalpy change from saturated liquid state to saturated vapor state	Btu/hr	4.33×10^7	$4.33x\ 10^7$
Total rate of enthalpy change on Working fluid side	Btu/hr	5.09×10^7	$5.19x\ 10^7$
Surface area required for preheat of Working fluid (from inlet to saturated liquid)	ft^2	62,000	59,401
Surface area required for vaporization of Working fluid (saturated liquid to saturated vapor)	ft^2	320,000	289,850

From table 9, it is clear that the flue gas velocity is higher in sub case-2 when compared to sub case-1 and it leads to increase in pressure drop of flue gas. The flue gas pressure drop is calculated using two approaches. Detailed description about pressure drop calculations can be found in Hazell's thesis (4). The working fluid pressure drop decreases with S_t because the required length of heat exchanger also decreases with decrease in transverse spacing.

Table 9 - Pressure drop calculations in NGCC case

	Units	Sub case -1	Sub case -2
Flue gas velocity	ft/s	15.0-13.7	18.5-16.9
Flue gas pressure drop (Incropera)	psi	0.0397	0.053
Flue gas pressure drop (Idelchik)	psi	0.0304	0.052
Working fluid pressure drop	psi	15.72	6.94

Table 10 - Cost calculations in NGCC case assuming whole tube bank is made of *carbon steel* irrespective of water condensation

	Units	Sub case -1	Subcase -2
Stainless steel tube Cost	$mil	0	0
Carbon steel tube Cost	$mil	2.33	2.11
Manufacturing & Installation cost	$mil	9.11	8.25
Total capital cost	$mil	11.44	10.36
Annual fixed cost	$mil	1.08	0.98
ID fan power	kW	11.77	17.61
Cooling fluid pump power	kW	10.16	4.49
Total power	kW	21.93	22.1
Annual operating cost	$mil	0.009	0.009
Total annual cost	$mil	1.09	0.99

Table 11 - Cost calculations in NGCC case assuming *stainless steel* tube bank is used when water condensation takes place

	Units	Sub case -1	Sub case -2
Stainless steel tube Cost	$mil	0.09	0.04
Carbon steel tube Cost	$mil	2.30	2.1
Manufacturing & Installation cost	$mil	9.11	8.25
Total capital cost	$mil	11.50	10.39
Annual fixed cost	$mil	1.09	0.983
ID fan power	kW	11.77	17.61
Cooling fluid pump power	kW	10.16	4.49
Total power	kW	21.93	22.1
Annual operating cost	$mil	0.009	0.009
Total annual cost	$mil	1.10	0.992

The cost calculations are done assuming the type of metal used in the tube bank is carbon steel in one case which can be observed in table 10. In other case, it was assumed that the tube bank is made of carbon steel in the absence of water condensation and stainless steel is used when water condensation takes place. The cost calculations for the latter case are shown in table 11. Stainless steel tubes are generally used in the applications where condensation of water is higher. It is assumed that there is no acid condensation from the flue gas in both NGCC and NGCC with cogeneration cases. The annual fixed cost is lesser in sub case -2 as it is proportional to the length of heat exchanger. The operating cost is almost same in both the sub cases. ID fan power, which is directly related to flue gas pressure drop, is higher in sub case-2 but this increment was offset by the cooling fluid pump power which is lower in sub case-2.

The cost difference between heat exchangers with and without stainless steel tubes is very low. The condensation of moisture in flue gas takes place almost near the exit of flue gas from heat exchanger duct. Considering the information related to moisture condensation point from table 6, it is clear that almost 98% of heat exchanger tubes are made of carbon steel and remaining 2% are stainless steel tubes. Substitution of 2% carbon steel tubes with stainless steel tubes doesn't have noticeable effect on the overall cost of heat exchanger. Thus, it is beneficial to have stainless steel tubes which are resistant to corrosion due to water condensation from flue gas in the heat exchanger.

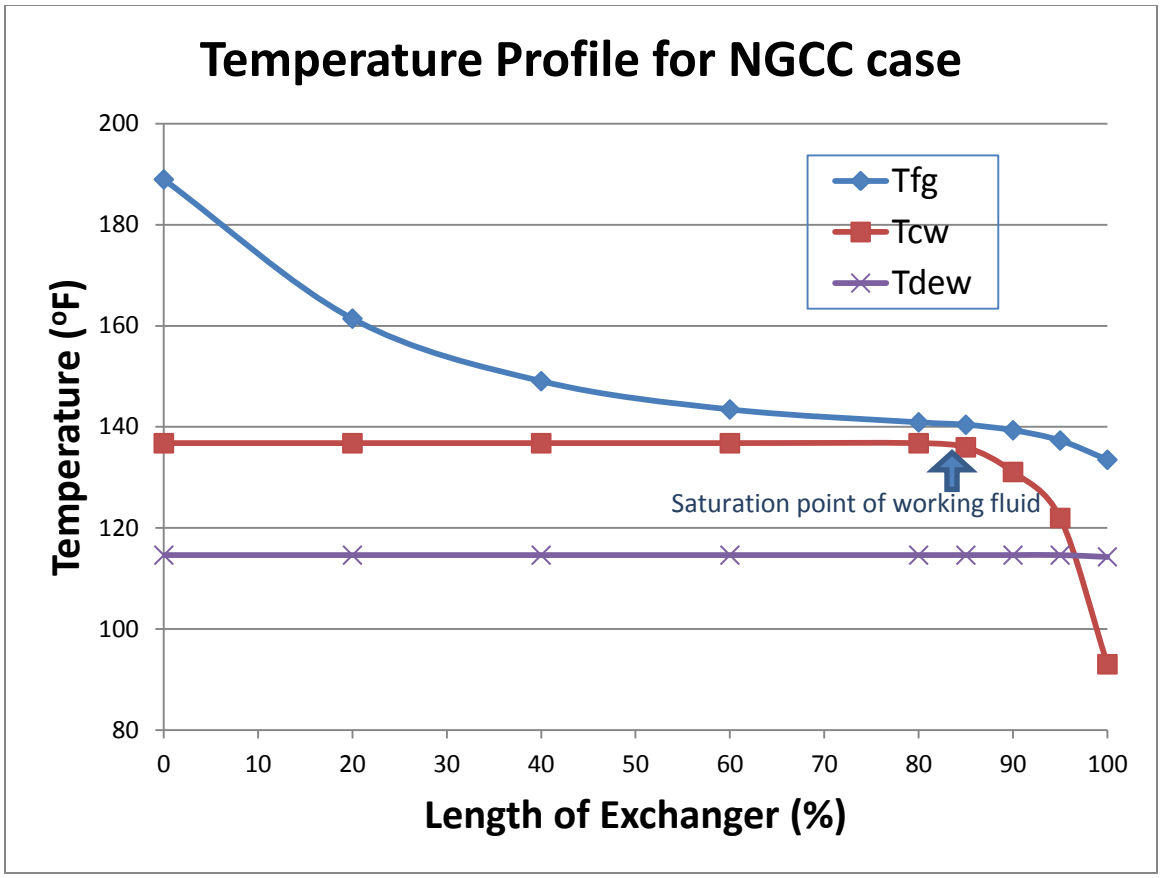

Figure 15 - Temperature profile for NGCC case

4.2 Pulverized coal case

In this case, coal is the source of flue gas. Simulations with three different transverse spacings are performed in this case. All the trends of various parameters mentioned in the NGCC case are applicable in pulverized coal case as well. The magnitudes of most of the parameters like heat transfer rates, pressure drop values and costs are higher in pulverized coal case.

Table 12 - Working conditions (inputs) for Pulverized coal

	Units	Magnitude
Flue gas inlet temperature	^{o}F	313
Flue gas flow rate	lbm/hr	6,736,000
Working fluid inlet temperature	^{o}F	80
Working fluid flow Rate	lbm/hr	2,9555,730
Working fluid to flue gas flow rate ratio	-	0.4387
Working fluid inlet pressure	psia	189.5
Working fluid exit temperature (saturated vapor)	^{o}F	214.65
Inlet mole fraction of water vapor in flue gas	-	0.10

Table 13 - Design data of heat exchangers used in Pulverized coal case

	Units	Sub case - 1	Sub case -2	Sub case -3
Duct height	ft	40	40	40
Duct depth	ft	40	40	40
Duct length	ft	69.65	53.73	38.90
Tube outer diameter	in	2.375	2.375	2.375
Transverse spacing, S_t	in	**4.75**	**4.0**	**3.3**
Longitudinal spacing, S_l	in	2.97	2.97	2.97
Total surface area of tube bank	ft^2	688,460	633,160	555,460

Table 14 - Flue gas parameters calculated in Pulverized coal case

	Units	Sub case - 1	Sub case -2	Sub case -3
Exit Flue gas (FG) Temperature calculated	^{o}F	154.35	153.79	153.16
Sensible heat transfer rate from FG	Btu/hr	2.90×10^8	2.91×10^8	2.92×10^8
Latent Heat Transfer rate from FG due to moisture condensation	Btu/hr	0.16×10^8	0.15×10^8	0.14×10^8
Total Heat Transfer rate from FG	Btu/hr	3.06×10^8	3.06×10^8	3.06×10^8
H2O condensation start point (in % of total length)	-	97.73	97.64	97.61
Calculated Duct length	ft	69.65	53.73	38.90
H2O condensation start point, L[ft] (as 0< L< Duct Length)	ft	68.07	52.47	37.975

Table 15 - Working Fluid parameters calculated in Pulverized coal case

	Units	Sub case -1	Sub case -2	Sub case -3
Working fluid (WF) rate of enthalpy change from inlet saturated liquid state	Btu/hr	1.37×10^8	1.37×10^8	1.37×10^8
WF rate of enthalpy change from saturated liquid state to saturated vapor state	Btu/hr	1.69×10^8	1.69×10^8	1.69×10^8
Total rate of enthalpy change on WF side	Btu/hr	3.06×10^8	3.06×10^8	3.06×10^8
Surface Area required for Preheat of WF (from inlet to saturated liquid)	ft^2	359,460	333,550	258,850
Surface Area required for Vaporization of WF(saturated liquid to saturated vapor)	ft^2	329,010	299,550	296,600

Table 16 - Pressure drop calculations in Pulverized coal case

	Units	Sub case -1	Sub case -2	Sub case -3
Flue Gas velocity	ft/s	44.1-35.0	54.1- 43.1	77.0-61.0
Flue Gas pressure drop (Incropera)	psi	0.422	0.6	1.14
Flue Gas pressure drop (Idelchik)	psi	0.458	0.75	1.45
Cooling Fluid pressure drop	psi	284.3	163.4	87.624

In the pulverized coal case, the cost calculations are done assuming the tube bank is made of nickel (Ni-22) alloy in table 18 and carbon steel in table 17. The type of tube material used when water condensation takes place is assumed to be stainless steel. Since the flue gas formed from coal combustion might contain vapors of acid, there might be a chance of acid condensation to take place. Nickel alloy is resistant to corrosion due to acid. So, the total cost of heat exchanger is estimated if heat exchanger with nickel alloy tube bank is used as an evaporator in an ORC.

The annual cost of evaporator with Ni 22 alloy tube bank is nearly 6 times higher than the evaporator with carbon steel tubes. If the flue gas has high mole fraction of sulfuric acid, then the corrosion due to acid deposition on carbon steel tubes might lead to replacement of whole tube bank. The cost of replacement and downtime of the evaporator might exceed the cost of heat exchanger with Ni 22 alloy tube bank. Further study is required to identify which type of tube bank in an evaporator is more beneficial in the case of pulverized coal.

Table 17 - Cost calculations in Pulverized coal case assuming *carbon steel* tube bank

	Units	Sub case -1	Sub case -2	Sub case -3
Carbon Steel tube Cost	$mil	4.13	3.80	3.33
Stainless steel tube Cost	$mil	0.185	0.156	0.083
Manufacturing & Installation cost	$mil	16.37	15.02	13.10
Total capital cost	$mil	20.70	18.98	16.52
Annual fixed cost	$mil	1.95	1.79	1.56
ID fan power	kW	309.41	471.84	901.72
Cooling fluid pump power	kW	912.29	524.32	281.18
Total power	kW	1221.7	996.15	1182.9
Annual operating cost	$mil	0.51	0.42	0.50
Total annual cost	$mil	2.46	2.21	2.06

Table 18 - Cost calculations in Pulverized coal case assuming *Ni 22 alloy* tube bank

	Units	Sub case -1	Sub case -2	Sub case -3
Ni 22 alloy tube Cost	$mil	119.8	110.06	96.54
Stainless steel tube Cost	$mil	0.185	0.156	0.083
Manufacturing & Installation cost	$mil	16.37	15.02	13.10
Total capital cost	$mil	136.36	125.24	109.72
Annual fixed cost	$mil	12.84	11.80	10.34
ID fan power	kW	309.41	471.84	901.72
Cooling fluid pump power	kW	912.29	524.32	281.18

Total power	kW	1221.7	996.15	1182.9
Annual operating cost	$mil	0.51	0.42	0.50
Total annual cost	$mil	13.35	12.22	10.84

From the temperature plot (Fig. 16), the working fluid becomes saturated liquid nearly at the midpoint of the heat exchanger. This implies that working fluid was in a state of liquid-vapor mixture in one half and it will be in a pure liquid state in the other half of heat exchanger. In the NGCC and NGCC with cogeneration cases, working fluid is in the state of liquid-vapor mixture in almost 80% of the heat exchanger.

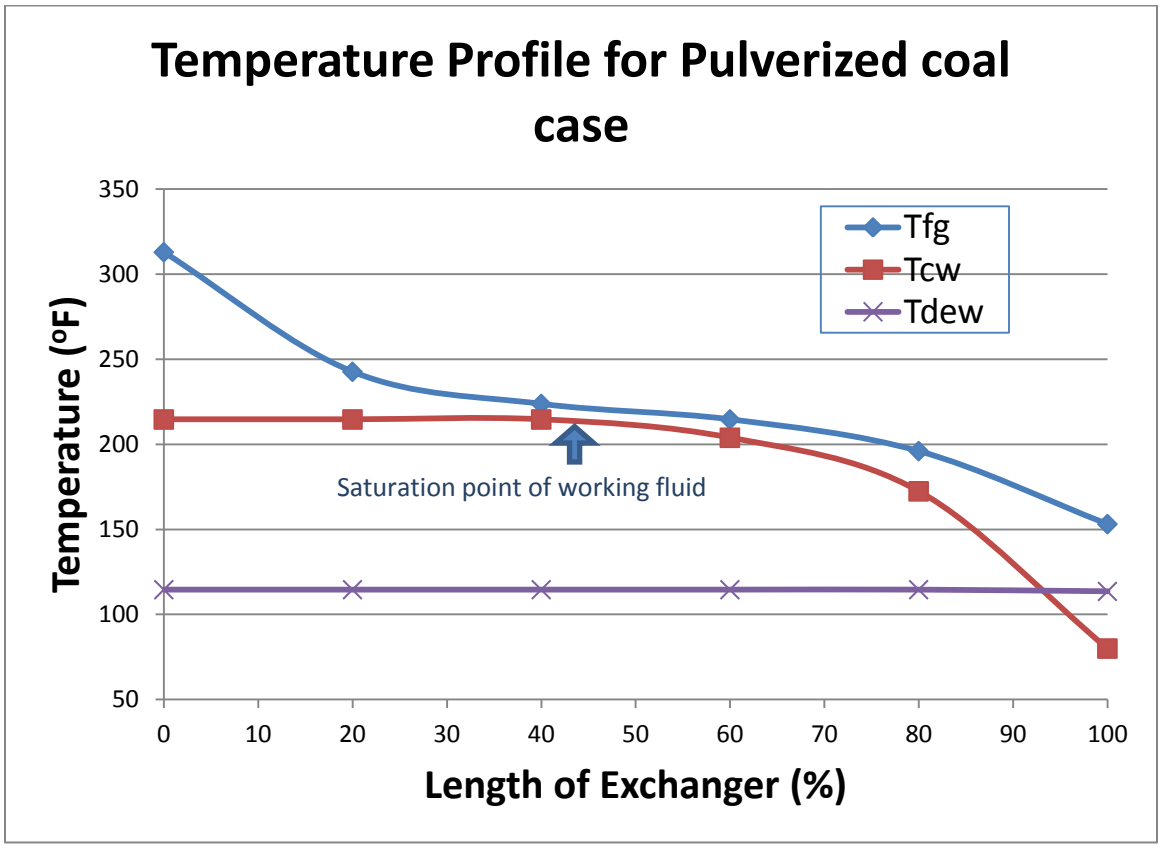

Figure 16 - Temperature profile for pulverized coal case

4.3 NGCC with Cogeneration case

The type of fuel used in this case is natural gas. Simulations are performed for three sub cases similar to the pulverized coal case. The working fluid flow rate and flue gas inlet temperature are higher in this case when compared to NGCC case. All the conclusions made in the NGCC case are applied for NGCC with cogeneration case as well.

Table 19 - Working conditions (inputs) for NGCC with Cogeneration

	Units	Magnitude
Flue gas inlet temperature	^{o}F	216
Flue gas flow rate	lbm/hr	3,353,000
Working fluid inlet temperature	^{o}F	96
Working fluid flow Rate	lbm/hr	814,153
Working fluid to flue gas flow rate ratio	-	0.2428
Working fluid inlet pressure	psia	74.25
Working fluid exit temperature (saturated vapor)	^{o}F	146.455
Inlet mole fraction of water vapor in flue gas	-	0.10

Table 20 - Design data of heat exchangers used in NGCC with Cogeneration case

	Units	Sub case - 1	Sub case -2	Sub case -3
Duct height	ft	40	40	40
Duct depth	ft	40	40	40
Duct length	ft	35.95	27.62	20.08
Tube outer diameter	in	2.375	2.375	2.375
Transverse spacing, S_t	in	**4.75**	**4.0**	**3.3**
Longitudinal spacing, S_l	in	2.97	2.97	2.97
Total surface area of tube bank	ft^2	355,350	324,700	286,900

Table 21 - Flue gas parameters calculated in NGCC with Cogeneration case

	Units	Sub case -1	Sub case -2	Sub case -3
Exit Flue gas (FG) temperature calculated	^{o}F	138.5	138.19	137.76
Sensible heat transfer rate from FG	Btu/hr	6.94×10^7	6.96×10^7	6.99×10^7
Latent Heat Transfer rate from FG due to moisture condensation	Btu/hr	0.21×10^7	0.19×10^7	0.18×10^7
Total Heat Transfer rate from FG	Btu/hr	7.15×10^7	7.16×10^7	7.17×10^7
H_2O condensation start point (in % of total length)	-	98.01	97.91	96.82
Calculated duct length	ft	35.95	27.62	20.08
H_2O condensation start point, L[ft] (as 0< L< Duct Length)	ft	35.24	27.04	19.45

Table 22 - Working Fluid parameters calculated in NGCC with Cogeneration case

	Units	Sub case -1	Sub case -2	Sub case -3
Working fluid (WF) rate of enthalpy change from inlet saturated liquid state	Btu/hr	1.36×10^7	1.36×10^7	1.36×10^7
WF rate of enthalpy change from saturated liquid state to saturated vapor state	Btu/hr	5.79×10^7	5.79×10^7	5.79×10^7
Total rate of enthalpy change on WF side	Btu/hr	7.15×10^7	7.15×10^7	7.15×10^7
Surface area required for preheat of WF (from inlet to saturated liquid)	ft^2	83,651	77,901	73,600
Surface area required for vaporization of WF(saturated liquid to saturated vapor)	ft^2	271,700	246,800	212,350

Table 23 - Pressure drop calculations in NGCC with Cogeneration case

	Units	Sub case -1	Sub case -2	Sub case -3
Flue gas velocity	ft/s	19.2-17.0	23.5-20.8	33.5-29.5
Flue gas pressure drop (Incropera)	psi	0.0545	0.076	0.15
Flue gas pressure drop (Idelchik)	psi	0.0538	0.088	0.175
Working fluid pressure drop	psi	12.69	7.45	4.17

Table 24 - Cost calculations in NGCC with cogeneration case assuming whole tube bank is made of *carbon steel* irrespective of water condensation

	Units	Sub case -1	Sub case -2	Sub case -3
Stainless steel tube Cost	$mil	0	0	0
Carbon steel tube Cost	$mil	2.14	1.96	1.7
Manufacturing & Installation cost	$mil	8.36	7.72	6.64
Total capital cost	$mil	10.51	9.53	8.34
Annual fixed cost	$mil	0.99	0.90	0.795
ID fan power	kW	18.34	28.16	54.22
Cooling fluid pump power	kW	11.22	6.84	3.80
Total power	kW	29.56	35.00	58.03
Annual operating cost	$mil	0.0124	0.015	0.0244
Total annual cost	$mil	1.00	0.915	0.814

Table 25 - Cost calculations in NGCC with cogeneration case assuming *stainless steel* tube bank is used when water condensation takes place

	Units	Sub case -1	Sub case -2	Sub case -3
Carbon steel tube Cost	$mil	2.139	1.958	1.69
Stainless steel tube Cost	$mil	0.0155	0.062	0.08
Manufacturing & Installation cost	$mil	8.36	7.72	6.64
Total capital cost	$mil	10.52	9.75	8.41
Annual fixed cost	$mil	0.991	0.918	0.81
ID fan power	kW	18.34	28.16	54.22
Cooling fluid pump power	kW	11.44	6.84	3.80
Total power	kW	29.79	35.00	58.03
Annual operating cost	$mil	0.0125	0.015	0.0244
Total annual cost	$mil	1.003	0.933	0.834

From the temperature profile of cogeneration case, it can be noticed that the working fluid is in liquid-vapor mixture state approximately within 74% of the total length of heat exchanger.

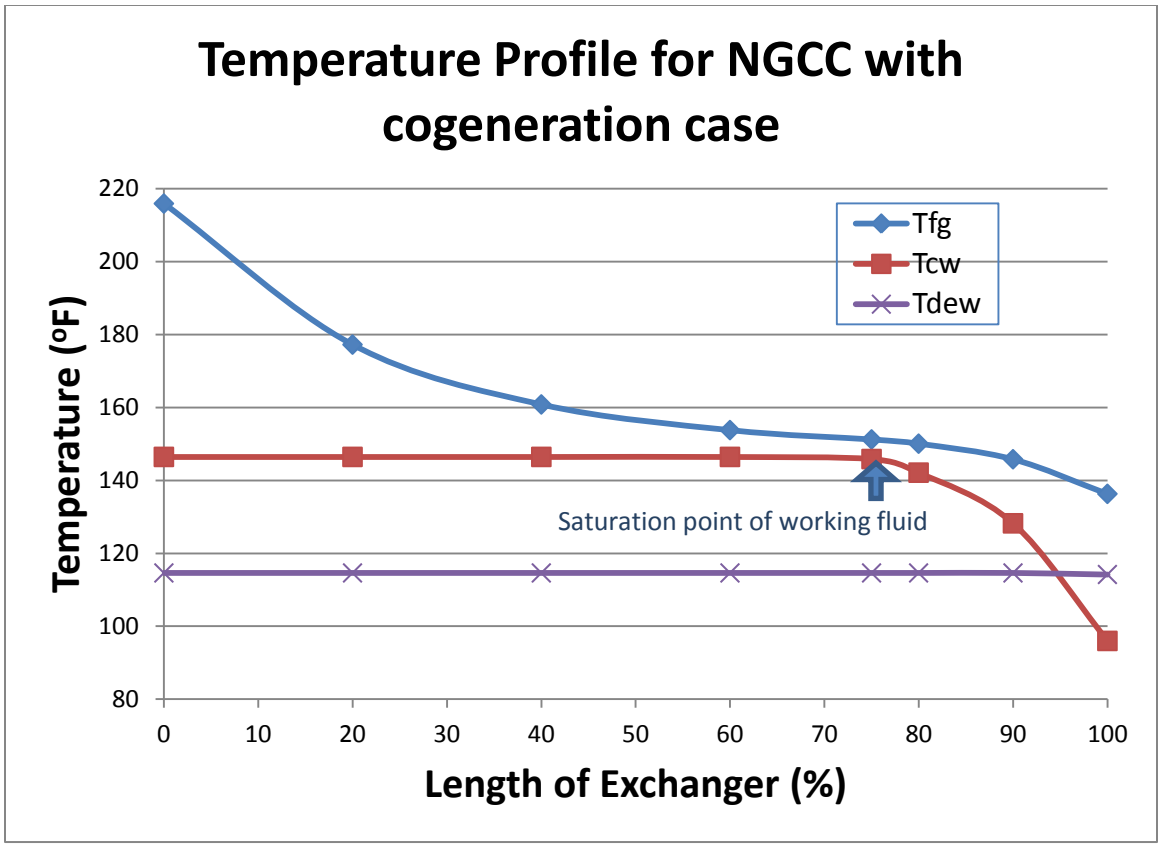

Figure 17 - Temperature profile for NGCC with Cogeneration case

For a comparative study, the results of simulations performed using ASPEN by the ERC researcher Charles were considered. The exit temperatures of flue gas in all the three cases calculated using ASPEN and the code were compared in the table given below.

Table 26 - Results agreement with simulations using ASPEN and ORC code

	Flue gas exit temperature (°F)		
	ASPEN	**ORC code**	**% deviation**
NGCC	128.25	133.32	3.05
Pulverized Coal	142.99	153.77	7.01
NGCC with Cogeneration	132.69	138.15	3.95

The ASPEN software calculates the parameters using the principles of energy balance and mass balance. It doesn't consider the geometry of heat exchanger and configuration of tubes. The results given by ORC code were based on the principles and assumptions mentioned in chapter-2. Also, the ORC code takes the design of heat exchanger into consideration unlike ASPEN.

5. CONCLUSION

Modeling the condensation of sulfuric acid present in flue gas on the tubes of full scale condensing heat exchanger was done using MATLAB. Simulations were performed based on three types of coals to calculate the sulfuric acid condensation rates and temperature profiles were plotted. The condensation rate of sulfuric acid decreases throughout the length of heat exchanger similar to the water condensation. Also, condensation rate is directly related to the mole fraction of sulfuric acid present in the flue gas.

The Organic Rankine cycle (ORC) is one possible method to recover the waste heat from flue gas and generate power. As a part of study to optimize the ORC system to achieve the best ratio of heat recovery to overall cost, the author's work focused on the study of evaporator used in the ORC. A computer program for heat exchanger which is used as evaporator in the ORC system was developed. Given, the inlet temperatures and flow rates of flue gas and working fluid, the code outputs the required length of heat exchanger, pressure drop values on both flue gas side and working fluid side and the overall cost of heat exchanger. It has been assumed that working fluid will exit the evaporator as a saturated vapor. Simulations were performed for 3 different ORC systems. The temperature profiles, the point of condensation of moisture in the heat exchanger and saturation point of working fluid were calculated for each case apart from the outputs mentioned above.

The type of tube material can be different in different applications based on the condensation of moisture and acid present in flue gas. Carbon steel tubes would be the lowest

cost but it would be subjected to acid corrosion. In the absence of acid and water condensation, carbon steel tubes are used. Stainless steel 304 would be the best material when water vapor condensation takes place. Nickel-22 alloy tubes have low corrosion rates due to acid condensation (4). The costs associated with different types of materials of tube bank were also assessed and the overall cost of heat exchangers in various applications was calculated using the code.

The assumption of working fluid exiting the heat exchanger as a saturated vapor can be overcome by implementing the properties of super heated working fluid and modify the energy balance equations in the computer program. This could be the future scope of the work done by the author.

REFERENCES & BIBLIOGRAPHY

1. **The Babcock & Wilcox Company.** *Steam.* Barberton : The Babcock & Wilcox Company, 2005. 41.

2. **Bourji, A., and Winstead,A.** Optimizing an Organic Rankine Cycle. *AIChE.* [Online] January 2013.

3. **Jeong, Dr. Kwangkook.** *Condensation of Water Vapor and Sulfuric Acid in Boiler Flue Gas.* s.l. : Lehigh University, 2008.

4. **Hazell, Daniel.** *Modeling and Optimization of Condensing Heat Exchangers for Cooling Boiler Flue Gas.* Bethlehem, PA : Lehigh University, 2011.

5. **Goel, Nipun.** *Design and Performance Analyses of Condensing Heat Exchangers for Recovering Water and Waste Heat from Flue Gas.* Bethlehem, PA : Lehigh University, 2012.

6. *Design of cooler condensers for Mixtures of Vapors with Noncondensing Gases.* **Colburn, A P and Hougen, O A.** s.l. : Industrial and Engineering Chemistry, Vol. 26.

7. **Zukauskas, A.** Heat Transfer from Tubes in Cross Flow. [book auth.] J P Hartnett, T F Irvine and Eds. Jr. *Advances in Heat Transfer.* New York : Academic Press, 1972.

8. **Gnielinski, V.** s.l. : Int. Chem. Eng., 1976, Vols. 16, pp 359-368.

9. **Petukhov, B.S.** [book auth.] J P Hartnett, T F Irvine and Eds. Jr. *Advances in Heat and Mass Transfer Vol. 6.* New York : Academic Press, 1970.

10. *Thermodynamique - Tensions des vapeurs: nouvelle relation entre les tensions et les temperature.* **Antoine, Ch. M.** s.l. : Comptes Rendus des Seances de l'Academie des Sciences, 1888, Vol. 104.

11. *A Method for Calculating Acid Deposition Rates in Regenerative Air Preheaters.* **D'Agostini, M. D.** s.l. : Proceedings of National Heat Transfer Conference, 1989.

12. **D'Agostini, Mark Daniel.** *Analysis of Sulfuric Acid Condensation in a Rotating Regenerative Air Preheater.* s.l. : Lehigh University, 1987.

13. **Valencia, Maria Pla Perujo aus.** *Condensation of Water Vapor and Acid Mixtures from Exhaust Gases.* s.l. : Technical University of Berlin, 2004.

14. **Munson, Bruce R., Young, Donald F. and Okiishi, Theodore H.** *Fundamentals of Fluid Mechanics.* s.l. : John Wiley & Sons, Inc., 1998. ISBN 0-471-35502-X.

15. *Estimating Costs of Shell-and-Tube Heat Exchangers.* **Purohit, G. P.** s.l. : Chemical Engineering, 1983, Vol. 90.

16. *Chemical Process Design and Integration.* **Smith, Robin.** Hoboken : Wiley, 2005.

VITA

Rinosh Polavarapu was born on April 3rd, 1989 in Vijayawada, India. He attended Birla Institute of Technology and Science (BITS) Pilani, Goa to pursue his undergraduate studies in 2006. He worked in Vestas R&D, Chennai and PMF engineering, Hyderabad from July 2010 to May 2011 as a part of the internship. After receiving the bachelor's degree in 2011, he joined Lehigh University in the Fall of 2011 to pursue masters in mechanical engineering.